CANCER

Mutant CEBPA directly drives the expression of the targetable tumor-promoting factor CD73 in AML

Janus S. Jakobsen[1,2,3*†], Linea G. Laursen[1,2,3†], Mikkel B. Schuster[1,2,3†], Sachin Pundhir[1,2,3,4], Erwin Schoof[1,2,3], Ying Ge[1,2,3], Teresa d'Altri[1,2,3], Kristoffer Vitting-Seerup[4], Nicolas Rapin[1,2,3,4‡], Coline Gentil[1,2,3], Johan Jendholm[1,2,3], Kim Theilgaard-Mönch[1,2,3,5], Kristian Reckzeh[1,2,3], Lars Bullinger[6], Konstanze Döhner[7], Peter Hokland[8], Jude Fitzgibbon[9], Bo T. Porse[1,2,3§]

The key myeloid transcription factor (TF), CEBPA, is frequently mutated in acute myeloid leukemia (AML), but the direct molecular effects of this leukemic driver mutation remain elusive. To investigate *CEBPA* mutant AML, we performed microscale, in vivo chromatin immunoprecipitation sequencing and identified a set of aberrantly activated enhancers, exclusively occupied by the leukemia-associated CEBPA-p30 isoform. Comparing gene expression changes in human *CEBPA* mutant AML and the corresponding *Cebpa*^{Lp30} mouse model, we identified *Nt5e*, encoding CD73, as a cross-species AML gene with an upstream leukemic enhancer physically and functionally linked to the gene. Increased expression of CD73, mediated by the CEBPA-p30 isoform, sustained leukemic growth via the CD73/A2AR axis. Notably, targeting of this pathway enhanced survival of AML-transplanted mice. Our data thus indicate a first-in-class link between a cancer driver mutation in a TF and a druggable, direct transcriptional target.

INTRODUCTION

Recent advances in our ability to sequence cancer genomes have left us with the challenge of translating this knowledge into tailor-made therapies targeting the characteristics of individual tumors, a concept frequently termed precision medicine. To harness the potential of precision medicine, we will need to identify oncogenic driver mutations and understand how they sustain disease development and maintenance.

One of the best characterized cancer types is acute myeloid leukemia (AML), a heterogeneous group of hematopoietic clonal disorders characterized by rapid accumulation of immature myeloid blasts at the expense of normal hematopoiesis. Specific cancer driver mutations, which underlie the distinct molecular AML subtypes, are closely linked to therapy outcome and overall risk stratification (*1*–*3*). Frequently found classes of leukemia drivers include fusion proteins and mutations in NPM1 [Nucleophosmin (encoded by *NPM1*)], epigenetic modifiers, signaling pathways, and the spliceosome, as well as loss-of-function mutations in key myeloid transcription factors (TFs) (*1*).

Despite our detailed knowledge of AML genetics, treatment has remained largely unchanged for decades and survival rates are low (*3*). Exceptions are novel therapies exploiting the genetic abnormalities of specific subgroups to target specific molecular events driving malignant transformation. An example is treatment of patients with acute promyelocytic leukemia (APL) with all-trans retinoic acid (ATRA), which overrides the differentiation block facilitated by the t(15:17) encoded PML-RARA fusion (*4*). Such an advancement emphasizes the importance of functionally characterizing the molecular pathogenesis to find new AML subtype-specific targets.

The TF CEBPA is essential for normal myeloid differentiation (*5*, *6*) and is mutated in approximately 10% of AML cases (*7*–*9*). The intron-less *CEBPA* gene is transcribed into a single mRNA, which is translated into two isoforms by alternative start codon usage: the full-length version termed p42 and a shorter version termed p30 that lacks the full trans-activation potential of p42. A frequently occurring class of *CEBPA* mutations in AML harbor *CEBPA* N-terminal nonsense or frameshift mutations, resulting in the exclusive expression of the p30 isoform from the mutated allele. C-terminal in-frame mutations interrupt DNA binding and homodimerization properties of the proteins and often co-occur on a separate allele from the N-terminal mutations (*8*). This pattern of mutations produces p30/p30 homodimers as the functional CEBPA TF entity in CEBPA mutant AML (*10*).

Biallelic *CEBPA* mutant AML is associated with an overall favorable clinical outcome (*9*) and constitutes a defined patient subgroup, corroborated by genetic subclassification (*1*) and gene expression profiling (*7*). The leukemia has been successfully modeled by the *Cebpa*^{Lp30} mouse line (termed Lp30) that contains an endogenous *Cebpa* mutation, resulting in the ablation of p42 expression, precisely mimicking the N-terminal *CEBPA* mutations in patients with AML. As a consequence, mice homozygous for the Lp30 allele are characterized by a myeloid differentiation block in preleukemic animals. This condition subsequently progresses into myeloid hyperproliferation and ultimately leads to the development of an overt and transplantable AML (*11*).

CEBPA has both activating and repressive activities. Among the transcriptionally activated targets are the genes encoding the myeloid-specifying G-CSFr, GM-CSFr, and MPO (*12*–*14*). Conversely, loss of CEBPA causes derepression of *Cebpg* (*15*) and *Sox4* (*16*), both of which are crucial for maintaining leukemic cells in a dedifferentiated state. However, it is not understood how the specific loss of full-length p42, and hence, the preferential p30/p30 homodimer formation

[1]The Finsen Laboratory, Rigshospitalet, Faculty of Health Sciences, University of Copenhagen, Copenhagen, Denmark. [2]Biotech Research and Innovation Centre (BRIC), University of Copenhagen, Copenhagen, Denmark. [3]Danish Stem Cell Centre (DanStem) Faculty of Health Sciences, University of Copenhagen, Copenhagen, Denmark. [4]The Bioinformatics Centre, Department of Biology, Faculty of Natural Sciences, University of Copenhagen, Copenhagen, Denmark. [5]Department of Hematology, Rigshospitalet, Faculty of Health Science, University of Copenhagen, Copenhagen, Denmark. [6]Department of Hematology, Oncology, and Tumor Immunology, Charité University Medicine, Berlin, Germany. [7]Department of Internal Medicine III, University Hospital of Ulm, Ulm, Germany. [8]Department of Hematology, Aarhus University Hospital, Aarhus, Denmark. [9]Centre for Haemato-Oncology, Queen Mary University of London, London, UK.
*Present address: Symphogen A/S, Ballerup, Denmark.
†These authors contributed equally to this work.
‡Present address: Deloitte Consulting, Copenhagen, Denmark.
§Corresponding author. Email: bo.porse@finsenlab.dk

affect the gene regulatory landscape on a global level and ultimately drives leukemic progression.

In this study, we used a combination of gene expression and chromatin immunoprecipitation sequencing (ChIP-seq) analyses to decipher the direct regulatory function of p30 in AML. We compared highly purified populations of leukemic granulocytic monocytic progenitors (L-GMPs; Lin^- $cKit^+$ $Sca1^-$ $CD150^-$ $CD41^-$ $FcgRII/III^+$) from both leukemic Lp30 mice and patients with AML to their closest healthy counterpart, GMPs. Using this approach, we identified *Nt5e*, encoding the ectoenzyme NT5E/CD73, as specifically up-regulated in biallelic *CEBPA* mutant leukemia as a consequence of p30 binding to a normally silenced upstream enhancer. CD73 catalyzes the conversion of adenosine monophosphate (AMP) into immune-dampening adenosine and has been shown to provide an immune evasive microenvironment in solid tumors. Correspondingly, an anti-tumor effect has previously been demonstrated upon blockade of the enzyme in cancers with CD73 expression. Here, we validated CD73 as a tumor-promoting factor in biallelic *CEBPA* mutant AML that can be targeted by dual inhibition of CD73 and adenosinergic signaling through the A2A receptor (A2AR), suggesting a novel precise treatment modality for this AML subtype.

RESULTS

CEBPA isoforms occupy specific genomic regions associated with distinct epigenetic profiles in normal and leukemic GMPs

To investigate the action of the cancer-driving CEBPA-p30 isoform, we performed ChIP-seq for CEBPA on phenotypically defined GMPs from wild-type (WT) and leukemic Lp30 mice isolated using fluorescence-activated cell sorting (FACS) (fig. S1A). In contrast to the Lp30 mouse model, solely expressing p30, WT GMPs almost exclusively express the full-length p42 isoform of CEBPA (*11*). Thus, for simplicity, we will refer to CEBPA in WT GMPs as p42, although, in addition to the predominant p42/p42 homodimer, these cells retain low levels of p42/p30 heterodimers and p30/30 homodimers. CEBPA genomic occupancy (Fig. 1A) was used to identify and subdivide stringent sets of regions bound by CEBPA either exclusively in leukemic GMPs (p30 regions), in WT GMPs (p42 regions), or shared between both conditions (common regions) (total of 30,951) (Fig. 1B and data file S1); 87.7% of the CEBPA-bound regions are common, whereas 4.5 and 7.9% are p42 and p30 specific, respectively (Fig. 1, B and C). ChIP-seq of histone 3 lysine 4 monomethyl (H3K4me1) and histone 3 lysine 27 acetyl (H3K27ac) modifications was performed to assess the coverage level of these enhancer-associated marks in the three sets of CEBPA regions (Fig. 1A and fig. S1B). Quantification of H3K4me1 (associated with an open chromatin structure) and H3K27ac (associated with active regions) levels shows substantial decoration with both marks in the common regions and no difference between the Lp30 and WT conditions (Fig. 1, C and D). In comparison, p42-specific regions display an overall lower level of enhancer marks [P (H3K27ac common versus p42) = 2.9×10^{-151} and P (H3K4me1 common versus p42) = 4.6×10^{-164}] and, moreover, a significant drop in the H3K27ac and H3K4me1 marks between WT and Lp30 L-GMPs, suggesting that CEBPA binding is required to maintain the activity levels of the p42 regions. In contrast, the p30-specific regions exhibit high H3K27ac levels in WT GMPs, which are further increased in Lp30 L-GMPs (Fig. 1, C and D). This demonstrates that p30-specific CEBPA binding is found primarily in regions that are already open (H3K4me1) and active (H3K27ac) in WT GMPs and become further activated following leukemic transformation.

CEBPA target enhancers can be subdivided into early (LSK; Lin^-, $Sca1^+$, Kit^+ and preGM; pre–granulocyte-macrophage progenitors) or late (GMP and granulocyte) activity enhancers based on their histone mark patterns during normal hematopoiesis as defined previously (*6*). The p42 regions overlap more with late than with early enhancers in accordance with the classical role of CEBPA in granulopoiesis (*10*), whereas p30 regions show no overlap preference (Fig. 1E).

Gene expression profiling by RNA sequencing (RNA-seq) showed a substantial number of deregulated genes ($\log_2$ fold change > 0.58, $P < 0.05$ by edgeR, see Materials and Methods) with higher (2342 genes) or lower (2469) expression in Lp30 L-GMPs compared to WT GMPs (Fig. 1F and data file S2). In line with a loss of transactivation activity as a consequence of the truncated trans-activation domain (TAD) in p30 (fig. S1C) (*17*, *18*), genes associated with common regions are more frequently down-regulated (1600) than up-regulated (1191) when comparing the Lp30 L-GMPs to their GMP WT counterparts. For the p42 and p30 regions, gene expression changes are in accordance with the differences in overall enhancer histone mark levels at these regions. Hence, p42 regions are preferentially associated with down-regulated genes (308 versus 102 up-regulated), while p30 regions are more associated with up-regulated genes (359 versus 253 down-regulated), comparing the Lp30 L-GMPs to WT GMPs (Fig. 1F). Together, gene expression and histone mark pattern changes indicate that CEBPA predominantly acts as a transcriptional activator, both in the Lp30 and in the WT cells, in line with most previous studies on CEBPA in late granulopoiesis.

In conclusion, we identify genomic regions bound specifically by p30 in the leukemic condition. Binding of p30 at these regions leads to increases in enhancer mark levels and changes in gene expression, suggesting that p30 is initiating a unique transcriptional program, potentially influencing leukemogenesis.

Leukemia-specific CEBPA target enhancers are enriched for E-twenty-six (ETS) family motifs and low-affinity CEBPA sites

To elucidate the differential CEBPA binding and enhancer mark activity of the p30 and p42 isoforms, we examined the relative enrichment of known TF binding motifs at p42- and p30-specific regions using the common regions as a reference. TF motifs enriched in p30 regions compared to common regions are binding sites recognized by TFs belonging to either the CEBP or the ETS family (e.g., ELKs, ERG, ETSs, ETVs, GABP1, FEV, and FLI1) (Fig. 2A) (see data file S1 for the full list of motifs). Among the ETS factors, ERG, FLI1, and PU.1 belong to a core set of TFs previously shown to bind at a wide range of hematopoietic enhancers in the murine HPC-7 stem/progenitor cell line (*19*). Using these data, we demonstrated that binding of the ETS factors was selectively depleted at p42-specific regions, and ERG in particular displayed a high degree of overlap with common and p30-specific regions (Fig. 2B). Moreover, and in contrast to FLI1 and PU.1, global quantitative proteomics analysis demonstrated that ERG was selectively up-regulated in Lp30 L-GMPs compared to WT GMPs, hinting at a role for ERG in binding of p30 to the p30-specific regions (Fig. 2C and data file S3). Conversely, the sequences enriched at the p42 regions are binding sites for the basic region leucine zipper (bZip) domain–containing CEBPs, as well as the PAR bZip family members DBP, HLF, and TEF (Fig. 2A). Of these, several are expressed in WT GMPs, e.g., CEBPE, CEBPG, and

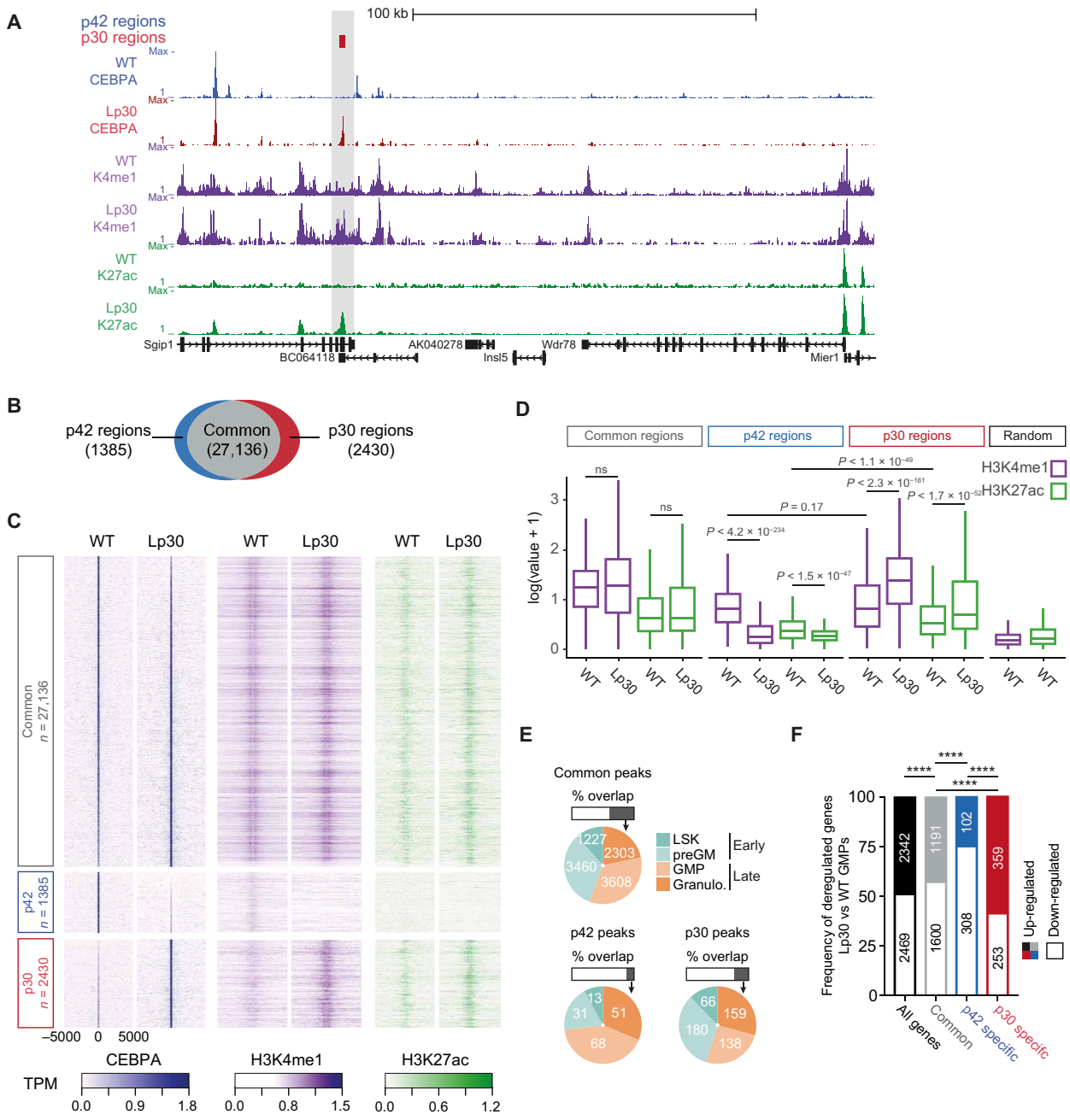

Fig. 1. Distinct enhancer binding of CEBPA in WT GMPs versus p30 L-GMPs. (**A**) Representative examples of CEBPA, H3K4me1, and H3K27Ac ChIP-seq tracks in WT GMPs and Lp30 L-GMPs, showing L-GMP p30-specific CEBPA binding. (**B**) Distribution of p42-specific, p30-specific, and common CEBPA-bound regions. (**C**) Normalized intensity tags per million (TPM) of CEBPA (left), H3K4me1 (center), and H3K27ac (right) at midpoint-centered enhancers [rows, ±5000 base pairs (bp)] across the three classes of regions in either WT GMPs or Lp30 L-GMPs. (**D**) Normalized intensity (TPM) for either H3K4me1 (purple) or H3K27ac (green) across the three classes of regions (midpoint-centered ±500 bp). "Random" represents all regions shuffled randomly across the genome. (**E**) Distribution of the three classes of regions into LSK-, preGM-, GMP-, and granulocyte-specific enhancers. (**F**) Subdivision of the three enhancer categories based on whether their nearest-neighbor genes are up- or down-regulated in Lp30 L-GMPs versus WT GMPs (log_2 fold change > 0.58, $P < 0.05$ by edgeR, see Materials and Methods). Statistics are two-sided Fisher's exact test between groups. ns, not significant.

CEBPZ (protein), as well as *Tef* and *Hlf* (mRNA). *Tef* is up-regulated, while *Hlf* is strongly down-regulated in Lp30 L-GMPs (Fig. 2D and data file S2). Thus, some of the loss of CEBPA binding at p42-specific regions might be explained by the loss of cobinding with HLF, as this factor has some occupancy overlap with the p42-specific regions (fig. S2A). Of the CEBP family members, CEBPA itself was strongly up-regulated (Fig. 2, C and D, and data file S3), which is consistent with previous findings in both human and murine *CEBPA* mutant AML (*11*, *20*). We validated these findings using quantitative reverse transcription polymerase chain reaction (RT-qPCR) (*Cebpa*; Fig. 2E) and Western blotting (CEBPA; Fig. 2F and fig. S2B).

To further probe the differential binding of the p30 and p42 CEBPA isoforms, we next compared the CEBPA motif scores (i.e., focusing only on bona fide CEBPA motifs) in each individual bound region

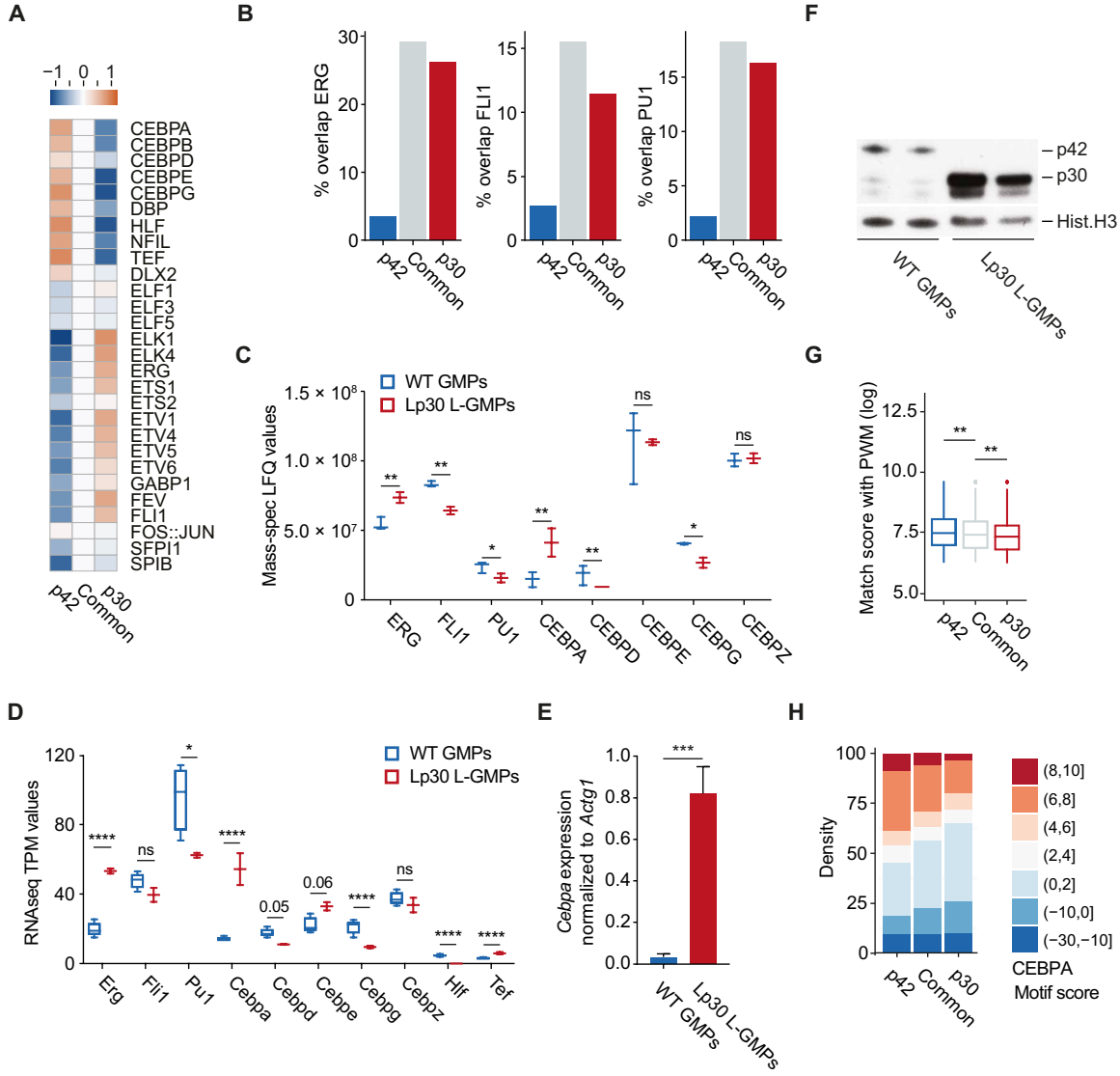

Fig. 2. Motif enrichment analysis of p42, common, and p30 CEBPA-bound regions. (**A**) TF motif enrichment analysis, combining results from three TF motif databases. The set of common regions is used as reference, and the relative enrichment *z* scores for p42 and p30 regions (compared to common) are displayed as shades of orange (enriched) or blue (depleted). (**B**) Percentages of CEBPA-bound regions overlapping with regions bound by ERG, FLI1, and PU1 in the HPC-7 cell line. (**C**) Proteomics quantification of TFs with enriched motifs, comparing FACS isolated WT GMPs and Lp30 L-GMPs (Limma multifactorial analysis, Benjamini-Hochberg corrected *P* value. $*P \leq 0.05$; $**P \leq 0.01$). (**D**) RNA-seq quantification of TF gene expression with enriched motifs, comparing WT GMPs and Lp30 L-GMPs (RNA-seq, *FDR ≤ 0.05; ****FDR ≤ 0.0001). (**E**) RT-qPCR quantification of *Cebpa* expression normalized to *Actg1* (WT GMPs, $n = 3$; Lp30 L-GMPs, $n = 7$, Student's *t* test. $***P < 0.001$). (**F**) CEBPA Western blot using WT GMPs and Lp30 L-GMPs. The CEBPA and Histone H3 bands were obtained from the same blot incubated with different Abs. (**G**) All CEBPA motifs found in p42, common, and p30 region sets tested for their match to the CEBPA consensus (Jasper DB. One-tailed Wilcoxon test. $**P \leq 0.001$). (**H**) Frequencies of bins of CEBPA-consensus matching motifs in each region set.

and found that, compared to the common regions, p42 regions, on average, harbor better matching motifs, while p30 regions display a lower average match score (Fig. 2G). Similarly, when we assess the CEBPA motif score distribution, CEBPA motifs associated with p30-specific regions are shifted toward low-scoring CEBPA motifs, compared to common and p42-specific regions (Fig. 2H), with both high- and low-scoring motifs conforming to CEBPA motifs (fig. S2C). These findings suggest that the increased CEBPA levels in Lp30 L-GMPs allow the p30 isoform to associate with low-affinity CEBPA sites.

Overall, our data indicate that CEBPA-p30–specific binding in Lp30 L-GMPs occurs at already active (H3K27ac marked) or at least open (H3K4me1 marked) enhancers. These enhancers are normally not bound by CEBPA in GMPs but are associated with other TFs such as ERG. We propose that increased levels of CEBPA in the Lp30 cells promote the binding of p30 to the low-affinity CEBPA motifs, leading to increased expression of a subset of associated genes.

Comparative analyses of murine and human CEBPA mutant AML pinpoints conserved transcriptional changes

We next set out to identify deregulated genes shared between human AML and the corresponding Lp30 mouse model, i.e., the shared core p30 leukemic transcriptional program, to identify gene expression

changes of potential clinical relevance. To this end, leukemic and normal GMPs from four patients with N/C-biallelic *CEBPA* mutant AML and two healthy volunteers, respectively, were isolated by FACS and subjected to RNA-seq (fig. S3A). Overall, fewer genes are deregulated ($\log_2$ fold change > 0.58, $P < 0.05$, edgeR, see Materials and Methods) in the human leukemic cells as compared to those of mice (data file S2), likely reflecting a higher level of biological variation in the human samples. More genes are down-regulated (2064) than up-regulated (1491) when comparing L-GMPs to normal GMPs (Fig. 3A).

Gene Ontology (GO) analyses revealed enrichment of many shared categories between human and mouse AML-associated gene expression changes (data file S4). Examples of categories significantly associated with up-regulated genes shared between the two species include "nucleosome core," "focal adhesion," "immunity," "apoptosis," and "negative regulation of cell proliferation." Similarly, many categories were shared between human and mouse down-regulated genes, including "cytoskeleton," "cell cycle," "cell junction"/"focal adhesion," "transcription," and "DNA damage" (Fig. 3B and fig. S3B).

To pinpoint conserved changes of individual genes, we generated a stringently filtered shortlist of genes for which a direct human or mouse ortholog could be identified and counted genes with aligned up- or down-regulation [using a cutoff of false discovery rate (FDR) < 0.01 for both edgeR and DEseq] (data file S2). Of the 415 (human) and 1778 (mouse) shortlisted genes, 102 were found to be regulated in the same direction, which corresponds to threefold more than expected by random distribution ($P < 0.0005$, Fisher's exact test) (Fig. 3C). Hence, these 102 genes constitute the core transcriptional program of *CEBPA* mutant AML and further demonstrate that the Lp30 mouse model mirrors key features of the corresponding human disease.

We next sorted the 102 genes associated with the *CEBPA* mutant transcriptional program based on expression fold changes in both species (Fig. 3D, left) and found that most were down-regulated (82 genes), while only 20 genes were up-regulated in Lp30 L-GMPs compared to normal GMPs. Notably, Gene Set Enrichment Analysis (GSEA) showed a strong overrepresentation of the 20 up-regulated genes and underrepresentation of the 82 down-regulated genes in biallelic *CEBPA* AML versus all other AMLs in the The Cancer Genome Atlas (TCGA) dataset (fig. S3C), supporting the notion of a subtype-specific core genetic program in human AML.

Normalizing expression changes individually for human and mouse samples (Fig. 3D, right), we found that only the top three genes, *ARPP21/Arpp1*, *NT5E/Nt5e*, and *ITGAX/Itgax*, were up-regulated from almost undetectable levels in healthy cells to high expression in leukemic cells derived from both species (data file S2). Of these, only *Nt5e* was significantly up-regulated at the protein level (NT5E/CD73) (Fig. 3E), while ARRP21 was not found by the proteomics analysis and ITGAX was not up-regulated (Fig. 3E and data file S3).

In summary, we have defined cross-species conserved core expressional changes induced by the CEBPA-p30 AML driver. Up-regulated genes, encoding potentially druggable proteins, were limited to a narrow set, in which *Nt5e* is an interesting candidate.

A leukemia-specific CEBPA-p30–bound enhancer controls Nt5e transcription

Nt5e encodes NT5E, ecto–5′-nucleotidase (aka CD73), an ectoenzyme that catalyzes the rate-limiting step of AMP to adenosine conversion. CD73 facilitates progression in several cancer types via (i) evasion of anti-tumor immune responses (*21*, *22*) and (ii) adenosine-mediated inhibition of apoptosis and promotion of proliferation of the tumor cells (*23*, *24*). Our demonstration of the conserved up-regulation of CD73 in p30-driven AML is therefore intriguing, and we sought to explore the connection further.

First, we validated the AML-specific expression of *Nt5e* mRNA and CD73 protein by independent methods in the Lp30 mouse model (Fig. 4, A and B). Having established a leukemia-specific expression of *Nt5e*, we investigated whether the aberrant expression of CEBPA-p30 in leukemic cells directly affects *Nt5e* levels. Scrutinizing the ChIP-seq data, we found that the p30-specific regions included a position 40 kb upstream of the *Nt5e* transcription start site (TSS), displaying clear CEBPA binding and enhancer-associated marks (H3K4me1 and H3K27ac) exclusively in the Lp30 cells, indicative of a leukemia-specific enhancer (Fig. 4C). Notably, this putative regulatory region is not decorated by H3K4me1 or H3K27ac histone marks at the granulocyte stage, suggesting that the enhancer mark is not due to premature differentiation of Lp30 L-GMPs (fig. S4A).

To investigate whether the putative −40-kb enhancer could regulate *Nt5e* expression, we first examined whether this region physically interacted with the *Nt5e* TSS using chromosome conformation capture (3C) with qPCR. Of seven tested regions spanning 50 kb upstream of *Nt5e*, we found two bordering the enhancer region interacting significantly with the TSS when comparing Lp30 L-GMPs to a cKit-enriched bone marrow (BM) control population, consistent with a direct physical contact between the −40-kb region and the *Nt5e* TSS (Fig. 4C, middle). We then applied CRISPR interference (CRISPRi) to assess the functional role of the −40-kb enhancer (*25*). To this end, we targeted two control positions (−112 and −15 kb, located distally from and in between the enhancer and TSS, respectively) and two enhancer positions, as well as the TSS with guide RNAs (gRNAs). This resulted in a significant reduction of *Nt5e* expression for enhancer-directed gRNAs equivalent to TSS targeting, compared to the controls (Fig. 4C, bottom). In contrast, no neighboring genes were significantly affected (fig. S4B). Last, we cloned the −40-kb region to a luciferase reporter vector and observed a small but significant induction of expression upon cotransfection with either CEBPA-p42 or the mutant p30 isoform (Fig. 4D). This supports the region's potential as a CEBPA targeted enhancer, activatable by either isoform when present at sufficient levels.

In combination, these data indicate that, in the Lp30 mouse model of *CEBPA* mutant AML, elevated levels of the p30 isoform directly drive expression of *Nt5e*. This is accomplished via a 40-kb upstream enhancer active exclusively in the malignant cells.

NT5E is overexpressed in CEBPA mutant AML patient samples and controlled by a CEBPA targeted enhancer

To test the potential clinical relevance of our findings in the Lp30 mouse model, we next wanted to extend them to human AML. To this end, we first carried out RT-qPCR and confirmed the high expression of *NT5E* found in our human RNA-seq data along with elevated levels of *CEBPA* (Fig. 5, A and B). Moreover, using flow cytometric analysis, we observed increased frequencies of GMP-resembling cells within the $CD3^-$ $CD19^-$ fraction (devoid of residual normal lymphocytes) of the $CD73^+$ population in patients with AML with biallelic CEBPA mutations (fig. S5A). These findings were further corroborated by analysis of three publicly available AML gene expression datasets, all demonstrating the high expression of *CEBPA* and *NT5E* in *CEBPA* mutant AML compared to other normal karyotype subtypes (Fig. 5C). The difference between *CEBPA* mutant and

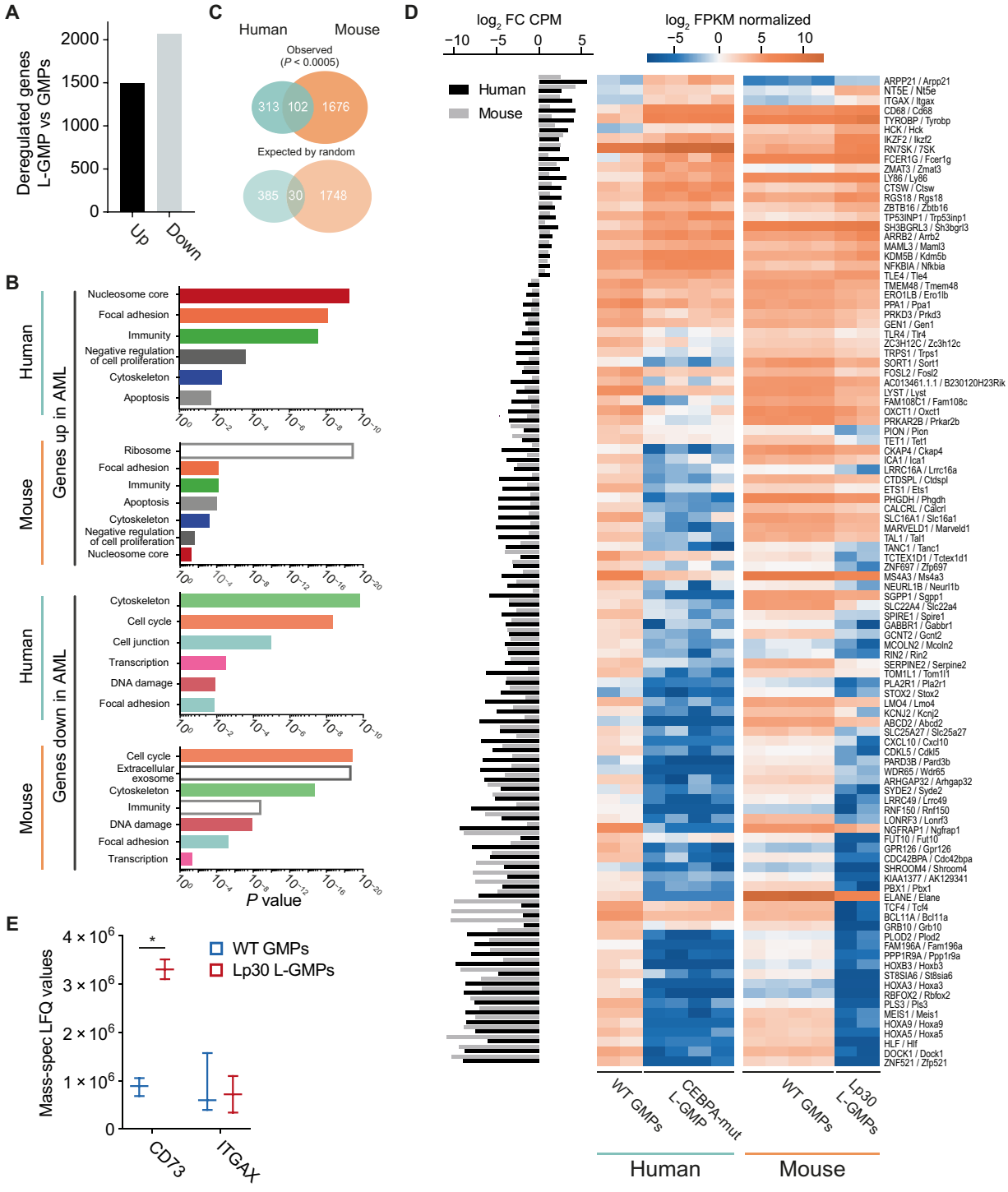

Fig. 3. Gene expression analysis of murine and human *CEBPA* mutant AML. (**A**) RNA-seq assessment of total up- and down-regulated transcripts in L-GMPs sorted from human AML samples with biallelic CEBPA mutations versus WT GMPs (log_2 fold change > 0.58, $P < 0.05$ by edgeR, see Materials and Methods). (**B**) Overrepresented GO categories (David online) of deregulated genes in L-GMPs versus normal GMPs. Included are representative, nonredundant categories found among the top 12 (up) or 64 (down) enriched in either species. "Negative regulation of cell proliferation" was included in AML-up for comparison to the down-regulated genes "cell cycle" category enrichment. "Transcription" was included for AML-down as it was enriched above the shared "DNA damage" in humans. Shared categories are colored; species specific are outlined in gray. See data file S4 for full list. (**C**) Stringently assessed deregulated mRNAs (FDR ≤ 0.01) in leukemic GMPs versus normal GMPs from human (teal) and murine (orange) BM. Lists of deregulated mRNAs were reduced to genes for which orthologs could be found in both species. Observed overlap (orthologs with shared directionality) (top) and expected random overlap (bottom) between the two species are indicated. (**D**) Quantified differential expression of the 102 overlapping genes shown in (C). Left: log_2 fold change for each species. Right: Relative expression levels normalized for each species individually. (**E**) CD73 and ITGAX protein levels assessed by mass spectrometry (MS) (Limma multifactorial analysis, Benjamini-Hochberg corrected *P* value. *$P \leq 0.05$).

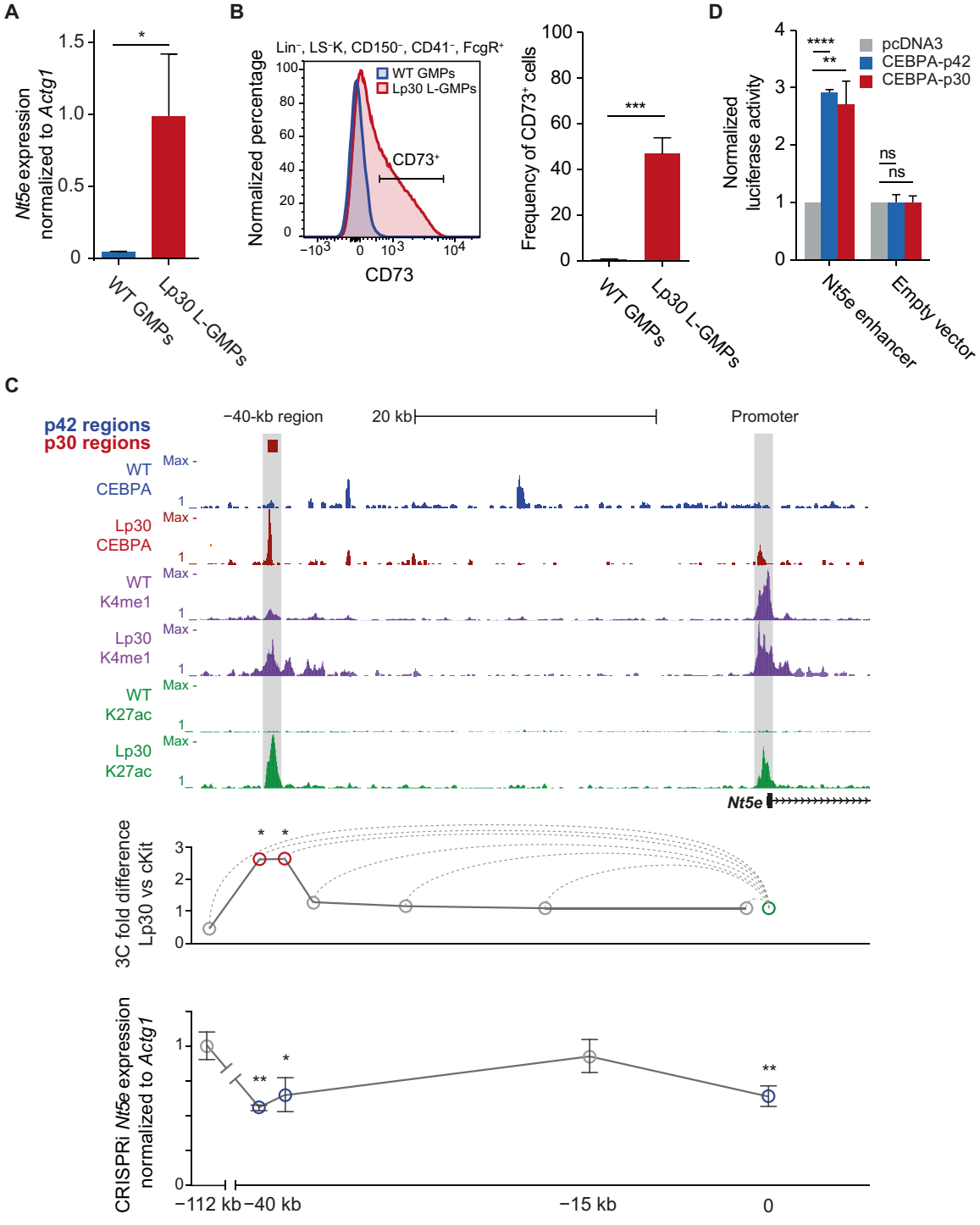

Fig. 4. CEBPA-p30 mediated activation of *Nt5e* expression. (**A**) RT-qPCR quantification of *Nt5e* expression normalized to *Actg1* (WT GMPs, $n = 3$; Lp30 L-GMPs, $n = 4$; mean ± SD, *t* test). (**B**) CD73 expression on the surface of WT GMPs and Lp30 L-GMPs as determined by flow cytometry (left) and the associated quantification CD73 expression GMPs (right; WT GMPs, $n = 2$; Lp30 L-GMPs, $n = 3$; mean ± SD, *t* test). (**C**) Top: ChIP-seq analysis on WT GMPs and Lp30 L-GMPs, showing a putative p30-specific enhancer located 40 kb upstream of the murine *Nt5e* gene. Middle: Assessment of direct interaction between the −40-kb enhancer and the *Nt5e* TSS by 3C-qPCR. Primer localization is depicted by open circles. qPCR ($n = 3$ to 5) was normalized to cKit–enriched BM cells (multiple *t* test, Holm-Sidak). Bottom: CRISPRi-mediated knockdown of *Nt5e* in Lp30 L-GMPs using gRNAs targeting the positions indicated by open circles. *Nt5e* expression was quantified by RT-qPCR, and expression levels were normalized to *Actg1* and to cells transduced with gRNA targeting position −112 kb [$n = 3$, mean ± SD, one-way analysis of variance (ANOVA) with Dunnett's correction, testing expression reductions between targeting enhancer or TSS positions versus the −112-kb control position]. (**D**) Dual luciferase assay assessing p42- or p30-mediated trans-activation of the −40-kb enhancer cloned upstream of a minimal promoter compared to an empty vector control ($n = 3$, mean ± SEM, *t* test). For all panels, $^{*}P \leq 0.05$; $^{**}P \leq 0.01$; $^{***}P \leq 0.001$; $^{****}P \leq 0.0001$.

other normal karyotype samples was most pronounced in the TCGA data, likely due to the lack of distinction between monoallelic and biallelic *CEBPA* mutant AMLs in the two older datasets (*26*, *27*). Last, we used RT-qPCR to test the expression of *NT5E* in a panel of defined AML subtype and healthy volunteer samples. Notably, we found that, apart from biallelic *CEBPA* mutant AML, *NT5E* expression was only consistently up-regulated in INV(16) AML (Fig. 5B). Analysis of a previously generated ChIP-seq dataset demonstrated that the CBFB-MYH11 fusion protein, associated with INV(16) AML, is located right at the NT5E promoter (fig. S5B) (*28*). These findings strongly suggest that *NT5E*/CD73 is specifically up-regulated by two leukemic driver mutations in their respective AML subtypes.

To elucidate the regulation of *NT5E* expression in human biallelic *CEBPA* mutant AML, we performed ChIP-seq for the H3K27ac histone mark on sorted GMP samples from either bi- or monoallelic *CEBPA* mutant AML patients or from healthy volunteers. Notably, a region 48 kb upstream of the human *NT5E* TSS displayed K27 acetylation in biallelic *CEBPA* mutant cells but neither in the monoallelic AML sample nor in healthy cells (Fig. 5D). Comparison with an external H3K4me1 and H3K27ac dataset from $CD34^+$ hematopoietic stem and progenitor cells (*29*) revealed enrichment for H3K4me1, but not for H3K27ac. This indicates that the −48-kb region is in an open but inactive state at the earliest phase of hematopoietic differentiation. Inspection of a comprehensive, human pan-hematopoiesis HiC study revealed that this region physically associates with the *NT5E* TSS in $CD8^+$ T cells (Fig. 5D, black and red bars) (*30*). Another publicly available ChIP-seq study showed the region to be marked by both H3K4me1 and H3K27ac in a similar T cell subset (Fig. 5D) (*31*), suggesting that, in these *NT5E*-expressing T cells, the region functions as an active enhancer driving *NT5E* transcription. Last, the −48-kb region gave rise to a small but significant increase in reporter activity in response to either p42 or p30 expression (Fig. 5E), indicating that CEBPA is able to function as a trans-activator at this region.

In short, our data show that both *CEBPA* and *NT5E* are specifically overexpressed in human biallelic CEBPA mutant AML. Our identification of an AML-specific −48-kb enhancer that can be activated by CEBPA suggests that CEBPA directly drives overexpression of *NT5E* in human *CEBPA* mutant leukemia, in line with the mechanism observed in the mouse model.

Down-regulation of Nt5e delays leukemia development in vivo

We next wanted to assess whether *Nt5e* played a tumor-promoting role in *CEBPA* mutant AML, and to this end, we applied short hairpin RNA (shRNA)–mediated knockdown of the gene (Fig. 6A). Lp30 cells transduced with retroviruses encoding either a scrambled (control) shRNA or one of two individual shRNAs targeting *Nt5e* along with a green fluorescent protein (GFP) marker were used for a competitive BM transplantation (BMT) assay (Fig. 6B). BM cells were harvested 4 weeks after BMT, and the GFP/YFP (yellow fluorescent protein) ratio of the leukemic cells was analyzed by flow cytometry analysis (Fig. 6C). *Nt5e* knockdown leukemic cells were efficiently outcompeted by competitor cells in comparison to the scrambled mix, thus establishing a tumor-promoting role of *Nt5e* in leukemia progression in vivo (Fig. 6D).

To further assess the effect of *Nt5e* knockdown on disease progression, we carried out a survival analysis on recipients transplanted with AML cells transduced with *shNt5e* or scrambled control. In accordance with the competitive assays, we found that shRNA-mediated *Nt5e* knockdown led to a significantly increased latency time compared to the scrambled control, with a median survival of 51.5 days for the scrambled control and 66.5 and 71 days for each of the shRNAs (Fig. 6E).

To rule out the possibility of off-target effects of the shRNAs, and to validate the ability of the enhancer to regulate *Nt5e* expression in vivo, we applied CRISPRi using gRNA constructs targeting either the *Nt5e* TSS or the −40-kb enhancer for transcriptional repression (Fig. 4C, bottom). Sublethally irradiated mice were transplanted with sorted Lp30 cells double positive for the KRAB-dCas9-mCherry and sgRNA-GFP expression vectors. Targeting either the *Nt5e* TSS or the −40-kb enhancer for transcriptional repression significantly increased survival of recipient mice compared to targeting the −112-kb control region (Fig. 6F).

Collectively, these results establish *Nt5e* as a critical factor for tumor progression in Lp30 AML. Importantly, our data also provide functional validation of the −40-kb *Nt5e* enhancer in vivo.

CD73 promotes tumor-protective adenosinergic autocrine signaling and is a potential therapeutic target in AML

Up-regulation of CD73 can cause an increased generation of extracellular adenosine. Accumulation of adenosine in the extracellular space signals through one or more of the four adenosine receptors: A1R, A2AR, A2BR, or A3R encoded by *Adora1*, *Adora2a*, *Adora2b*, and *Adora3* (*32*). RT-qPCR analysis of Lp30 and WT cell samples showed a specific and selective high expression of *Adora2a*, in comparison to *Adora1*, *Adora2b*, and *Adora3* in the Lp30 cells (Fig. 6G). Human biallelic *CEBPA* mutant AML also displays *ADORA2A*, *ADORA2B*, *and ADORA3* expression, again with *ADORA2A* being the highest, which is paralleled in human INV(16) AML (fig. S6A). In a cancer setting, adenosine signaling, in particular, via the A2AR, may contribute to tumor progression by modulating inflammatory processes, promoting proliferation, and inhibiting apoptosis of the cancer cells, mostly via activation of the intracellular cyclic adenosine monophosphate (cAMP) pathway (*33*).

To examine expression changes caused by knockdown of *Nt5e* in the Lp30 cells, we performed RNA-seq analysis on Lp30 leukemic cells transduced with *shNt5e* or scrambled control (data file S5). To test the hypothesis that adenosine generated by CD73 can have an auto- or paracrine effect on the leukemic cells through activation of A2AR, we curated a negative A2AR signature of downstream targets directly suppressed by A2AR signaling and calculated the signature enrichment alongside GO signatures identified using GSEA (data file S7). The negative A2AR signaling signature had the highest fold change between control and *Nt5e* knockdown Lp30 cells, followed by signatures associated with immune activation, responses that are affected by adenosine/cAMP signaling as well (Fig. 6H) (*34*). This suggests that targets normally repressed in Lp30 cell by A2AR signaling are indeed up-regulated by *Nt5e* knockdown, which supports the notion of an adenosinergic autocrine loop of signaling, promoted by CD73 in the Lp30 cells. Further, we queried the TCGA AML dataset by GSEA and found the A2A signature genes to be repressed in the biallelic *CEBPA*-mutated subtype versus all other subtypes (Fig. 6I), supporting the existence of subtype-specific signaling.

To directly assess the functional effect of A2AR signaling on cell growth, we measured the proliferation rates of Lp30 cells subjected to a specific A2AR inhibitor, SCH-58261. Cells treated with increasing concentrations of the inhibitor showed a dose-dependent decrease

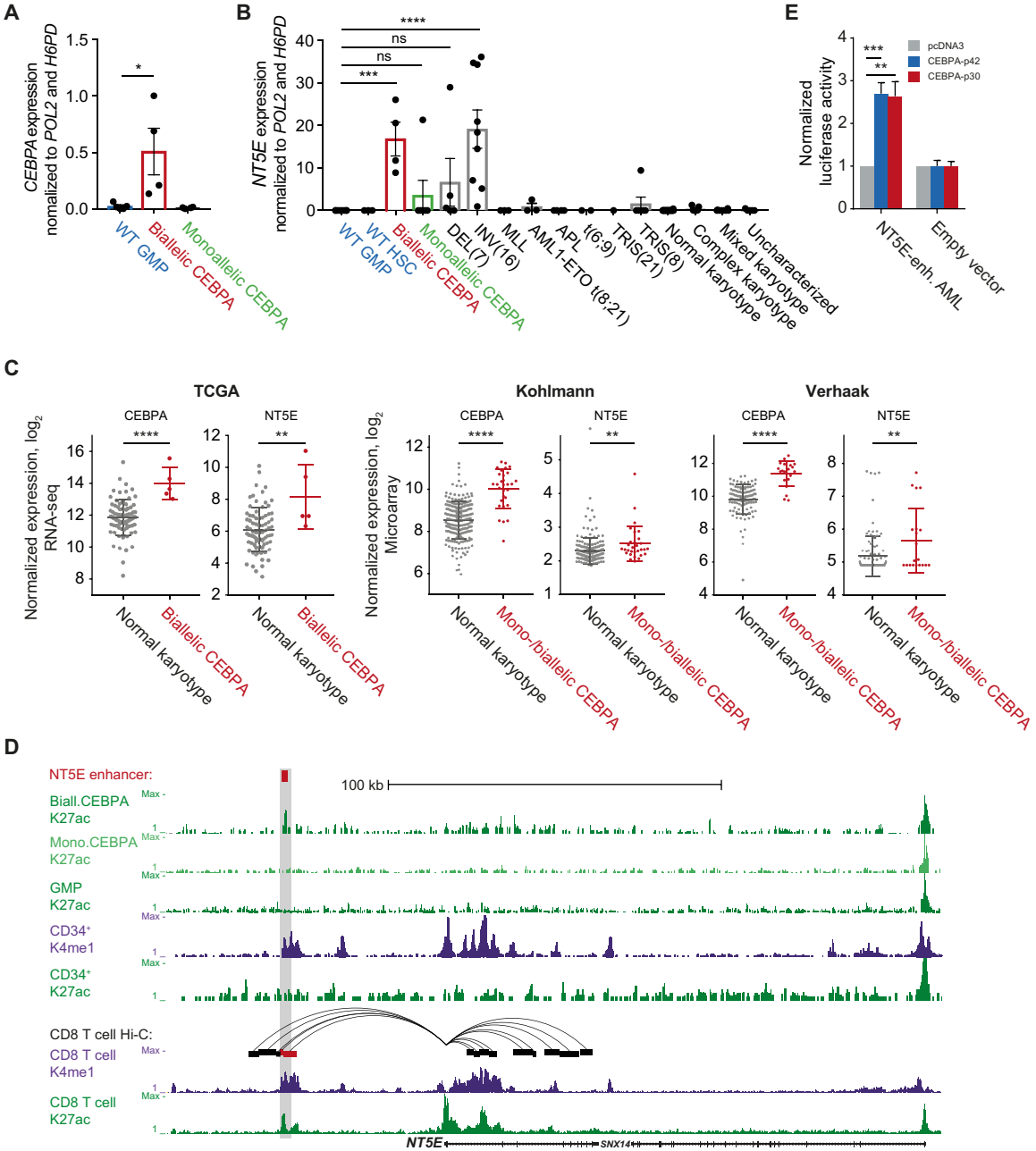

Fig. 5. Up-regulation of *NT5E* in human AML samples with biallelic *CEBPA* mutations. (**A**) RT-qPCR quantification of *CEBPA* mRNA in sorted GMPs from healthy individuals as well as patients with AML with monoallelic and biallelic CEBPA mutations. Normalized to *POL2* and *H6PD* ($n = 5$, 4, and 4, mean ± SEM). (**B**) RT-qPCR quantification of *NT5E* expression levels in sorted GMPs from healthy individuals and patients with AML with the indicated mutational status. Normalized to *POL2* and *H6PD* ($n = 8$, 3, 4, 6, 6, 9, 3, 3, 4, 4, 1, 6, 22, 7, 8, and 5, mean ± SEM). Statistical significance was assessed using one-way ANOVA with Dunnett's correction for (A) and (B), where the mean of each group was compared to the WT-GMP group. (**C**) Normalized expression of *CEBPA* and *NT5E* in datasets extracted from the cBioPortal (TCGA data, RNA-seq) and Leukemia Gene Atlas (expression array) databases (mean ± SD). For Kohlmann and Verhaak datasets, the monoallelic and biallelic CEBPA-mutated subtypes are binned as one group, and for TCGA data, the biallelic subtype is separate. (**D**) Top: ChIP-seq analysis on GMPs from healthy individuals and L-GMPs from patients with AML with monoallelic and biallelic CEBPA mutations showing a putative enhancer located 48 kb upstream of the human *NT5E* gene. Center: ChIP-seq tracks from $CD34^+$ hematopoietic progenitor cells. Bottom: Publicly available Hi-C data in black and red bars (*30*) and ChIP-seq tracks (*31*) from the same region in CD8 T cells. (**E**) Dual luciferase assay assessing p42- or p30-mediated trans-activation of the −48-kb enhancer cloned upstream of a minimal promoter compared to an empty vector control ($n = 3$, mean ± SEM, Student's *t* test). For all panels, $^*P \le 0.05$; $^{**}P \le 0.01$; $^{***}P \le 0.001$; $^{****}P \le 0.0001$.

in growth rates (fig. S6, B and C). In comparison, murine leukemic Inv(16) cells with low A2AR expression were not affected, demonstrating the requirement for A2AR (fig. S6, D and E). Analyses of A2AR inhibitor–treated Lp30 cells revealed a significant >2-fold decrease of cells in the S-G_2-M phase (fig. S6, F, G, and H) and a marked increase of apoptotic cells (sub-G_1 or annexin V marked) compared to the control (fig. S6, G and I).

Studies on solid cancer models have demonstrated anti-tumor effects of inhibiting CD73 activity with specific blocking monoclonal Abs (mAb) or using genetic knockdown (*35*–*39*). Expression of A2AR

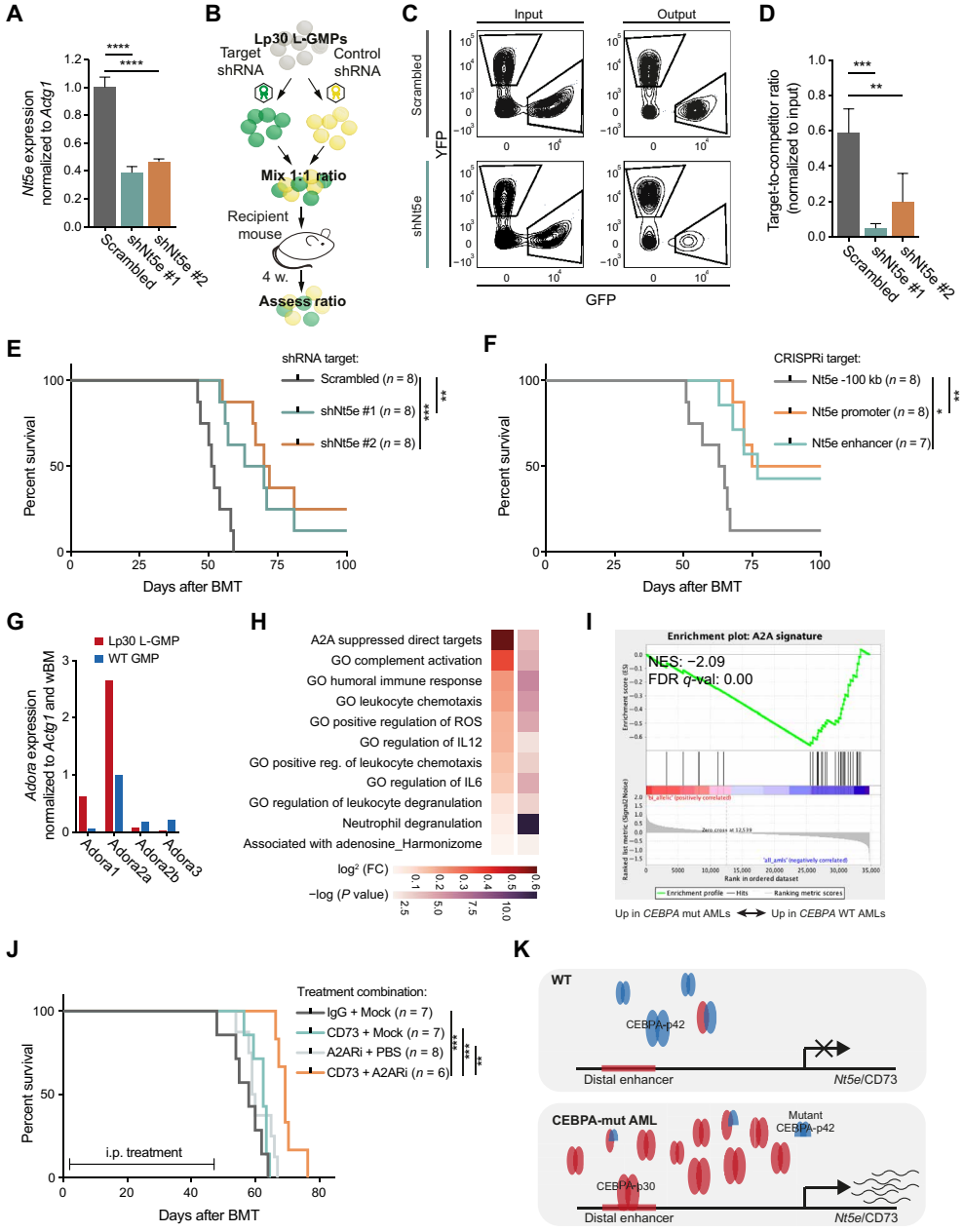

Fig. 6. Effect of *Nt5e* KD on in vivo AML progression and identification of CD73 tumor-protective adenosinergic signaling as a potential therapeutic target. (**A**) *Nt5e* knockdown efficiency; RT-qPCR quantification of *Nt5e* normalized to *Actg1*. GFP$^+$ sorted Lp30 cells transduced with *shNt5e* or scrambled control ($n = 3$, mean ± SD). (**B**) Schematic outline of competitive BM transplant experiment. (**C**) Representative FACSs of Lp30 cells transduced with shRNA targeting *Nt5e* or scrambled control at the input and output time points. (**D**) Target-to-competitor (GFP/YFP) ratio of Lp30 cells transduced with shRNA targeting *Nt5e* or scrambled control after BMT and 4 weeks of leukemia progression. Ratio was normalized to input cells. ($n = 4$, mean ± SD). (**E**) Survival of recipient mice transplanted with 2.5×10^4 GFP$^+$-sorted Lp30 cells transduced with *shNt5e* or scrambled control ($n = 8$). (**F**) Survival of recipient mice transplanted with 5×10^3 cells double positive for KRAB-dCas9-mCherry and sgRNA-GFP targeting *Nt5e* TSS, a putative enhancer (−40 kb), or a negative upstream region (−100 kb) ($n = 7$ and 8). (**G**) RT-qPCR quantification of *Adora1*, *Adora2a*, *Adora2b*, and *Adora3* in Lp30 L-GMP and WT-GMP cells, displayed as ratios to levels in whole BM cells. Normalized for each cell type to *Actg1* (wBM, $n = 3$; GMPs, $n = 5$ to 6). (**H**) Signatures enriched in both *Nt5e* knockdown groups in vivo compared to scrambled control based on RNA-seq (Scr, $n = 3$; shNt5e #1, $n = 3$; shNt5e #2, $n = 2$). Color indicates $\log_2$ fold change (red) and *P* value (purple) for each signature. See data file S6 for full list. (**I**) Plot and statistical values from GSEA testing genes of the negative A2A signature in biallelic CEBPA-mutated AML versus all other AML subtypes; TCGA AML expression dataset. (**J**) Survival of recipient mice transplanted with 100 freshly harvested Lp30 cells. Mice were injected intraperitoneally with mock, A2ARi (SCH-58261, 20 μg), anti-CD73 (2C5-IgG2a, 100 μg), and control-Ig (NIP228-IgG2a, 100 μg) in combinations as indicated. Treatments were twice weekly from day 1 until the first mouse was euthanized, as specified on the graph. (**K**) Model of *Nt5e* differential leukemia-specific expression as a consequence of elevated CEBPA-p30, leading to engagement of the *Nt5e* AML enhancer. Blue ovals represent CEBPA-p42, and red ovals represent CEBPA-p30 monomers. Bottom: Half blue ovals represent CEBPA-p42 mutated in the DNA-binding domain, often present in human biallelic CEBPA-mutated AML. Statistics were determined by Student's two-tailed *t* test (two groups) or one-way ANOVA corrected for multiple comparisons (Dunnett's correction) between control and treatment groups (three or more groups) or log-rank test (survival). *$P \leq 0.05$; **$P \leq 0.01$; ***$P \leq 0.001$; ****$P \leq 0.0001$.

on myeloid cells is required for efficacy of CD73 inhibition (*40*). In addition, an additive effect of combining CD73 mAb with an A2AR inhibitor has been demonstrated in a breast cancer model (*39*). To test whether interruption of adenosine signaling in the Lp30 cells could halt AML progression in vivo, we transplanted recipient mice with Lp30 cells and treated them with either a CD73 mAb or the SCH-58261 A2AR inhibitor, or the combination of the two. Treatment with any of the agents as a monotherapy showed a trend toward increased survival time (median survival of 62 and 59.5 days for mAb or A2ARi, respectively), whereas the combination caused a significant increase in median survival time (69 days) over both immunoglobulin G (IgG) + Mock (58 days) and any of the treatments alone (Fig. 6J), supporting a favorable additive effect on survival by blocking different nodes of the adenosine signaling pathway.

Together, these results support the notion of leukemia-specific CD73-mediated production of adenosine to signal via A2AR, promoting proliferation and preventing apoptosis in a cell-autonomous manner. This tumor-protective autocrine signaling loop is likely initiated by the AML-specific CEBPA-p30 binding and activation of the novel distal enhancer of *Nt5e/NT5E* (Fig. 6K). The in vivo results point toward the potential therapeutic benefit of targeting the CD73/A2AR axis, thereby inhibiting the adenosinergic pathway.

DISCUSSION

Biallelic *CEBPA* mutant AML constitutes a distinct genetic and molecular subgroup within AML, elicited by the isoform shift from essentially p42-restricted expression to exclusive functional usage of the CEBPA-p30 AML driver (*10*). Characterization of the functional consequences of such oncogenic drivers is critical to develop new treatment regimens for AML subtypes, classically treated with nonspecific, cytotoxic chemotherapeutics. In this study, we found that differential chromatin occupancy of CEBPA directly influences transcriptional output in the leukemic condition. Moreover, we identified critical, tumor-promoting genes driven directly by the p30 isoform, at least partially explaining the underlying causal role of this isoform in leukemogenesis. To our knowledge, this is the first time that such a mechanism has been demonstrated for an oncogenic TF variant. Last, we describe the p30-dependent, and thus *CEBPA* biallelic-specific, up-regulation of *Nt5e* as a tumor-promoting factor and a potential therapeutic target.

Despite a high degree of shared specificity of p30/p30 homodimers in L-GMPs and p42/p42 homodimers (as well as small amounts of p42/p30 and p30/p30 dimers) in WT GMPs, a substantial number of binding sites showed differential binding between the two isoforms. Our computational motif enrichment search revealed that the p30-specific regions harbored relatively more low-affinity CEBPA binding sites than their shared and p42-specific counterparts. We suggest that, to a large extent, this can be explained by the increased expression of CEBPA in L-GMPs, which would allow CEBPA-p30 to associate with low-affinity binding sites. In addition, one could hypothesize that the loss and gain of alternative CEBPA interaction partners might influence site specificity. Of note, we observe that *Hlf* levels were reduced, while *Erg* display increased expression in the leukemic context. Concordantly, we found a substantial overlap between p42- and p30-specific binding and cognate binding sites for HLF and ERG, respectively. Further, we observed that p30-specific regions are defined by active enhancer marks, suggesting that p30 mainly binds chromatin that is already open. Conversely, p42-specific regions in WT GMPs displayed a relatively low openness as defined by H3K4me1 coverage, suggesting that these regions depend on the "pioneering" activity of full-length CEBPA (*6*, *41*) and that p30 does not retain this activity. This is emphasized by the fact that p42 binding overlaps relatively more with late enhancers, which depend on the pioneering capacity of this isoform (*6*). As for the correlation between CEBPA binding and gene expression changes, the common regions were generally associated with genes down-regulated in L-GMPs. This is probably accounted for by the absence of the N-terminal TAD1 in the p30 isoform, which has previously been shown to have the major trans-activation potential of the protein. Conversely, p30-specific binding is associated with leukemia-specific increases in gene expression, underscoring that the TAD2 is sufficient (albeit less efficient) for gene activation, potentially also by cooperating with other TFs, like ERG. Collectively, our analyses demonstrate that CEBPA-p30 controls an AML-specific transcriptional program through novel binding at already established enhancers, induced, in part, by the increased expression of the p30 isoform, and that modulation of CEBPA binding may potentially be influenced by other TFs such as ERG and HLF.

Previous work has identified *Cebpg* and *Sox4* as critical downstream targets of CEBPA in *CEBPA* silenced/*CEBPA* mutant AML, respectively (*15*, *16*). Both proteins are normally repressed by CEBPA and up-regulated in its absence and, in the case of SOX4, up-regulated by the expression of the p30 isoform as well. In line with this, we found that both p42 and p30 bind the promoters of both genes and that SOX4 is up-regulated in Lp30 L-GMPs (data not shown). One possible explanation for the derepression of these genes following the p42 to p30 isoform switch could be that repression depends on the previously reported selective association of p42 with HDAC1 and HDAC2 (*42*).

Overall, our data, together with previous studies, suggest that the isoform switch from p42 to p30 expression drives an AML-specific transcriptional program via several mechanisms, including (i) loss of CEBPA-driven gene expression at p42-specific loci, (ii) loss of p42-mediated repression at common sites, (iii) loss of transcriptional activity at common regions due to reduced transcriptional activity of the p30 isoform, and (iv) activation of already established enhancers via p30 binding to low-affinity sites mediated by its increased expression and potentially also by ETS factors such as ERG.

Although targeting of, *SOX4* and *CEBPG* may have a potential benefit in *CEBPA* mutant AML, TFs are generally not considered as good drug targets as cell-surface proteins or proteins harboring enzymatic activities such as kinases and epigenetic regulators. Here, we identified *Nt5e* as belonging to a transcriptional program driven by the p42 to p30 isoform switch in *CEBPA* mutant AML. We found *Nt5e* expression to be regulated by a p30-bound leukemic-specific enhancer in a manner that appears to be conserved across human and murine AML. Apart from *CEBPA* mutant AML, deregulated expression of *NT5E* was only consistently observed in INV16 AML, where the CBFB-MYH11 fusion protein locates directly to the promoter of *NT5E* and likely drives its expression. This demonstrates that *NT5E* up-regulation is tightly associated with specific oncogenic drivers. Down-regulation of *Nt5e* either by shRNAs or through CRISPRi using gRNAs targeting the TSS or the p30-bound −40-kb enhancer demonstrated a key role for CD73 as a tumor-promoting factor in *CEBPA* mutant AML.

CD73, together with CD39, catalyzes the formation of free adenosine on the surface of lymphocytes, endothelial cells, and a large

subset of primary tumors (*22*). By shifting the balance between the immune-activating ATP and immune-suppressing adenosine, CD73 has been proposed to protect cancer cells against the host immune system (*21*, *22*). We tested this concept for the Lp30 AML model by comparing the effect of *Nt5e* knockdown in immunocompromised NSG mice versus C57BL/6 mice or following T cell depletion. However, in neither case did a reduction in the host immune system interfere with the tumor-promoting effect of CD73 (data not shown), suggesting that CD73, in *CEBPA* mutant AML, protects tumor cells via another mechanism. Free adenosine may also act on tumor cells in a paracrine/autocrine manner via the adenosine receptors (*33*). In line with this, we found that treatment of Lp30 cells in vitro with an A2AR receptor antagonist halted cell cycle progression and induced apoptosis. Moreover, we found that down-regulation of *Nt5e* promoted the derepression of genes, which are normally inhibited by the stimulatory action of A2AR on the adenyl cyclase, one of its downstream targets. Thus, our observations are consistent with a mechanism where CD73-dependent adenosine acts on A2AR to sustain leukemic cell growth and protect against apoptosis, paralleling earlier reports using a model of chronic lymphocytic leukemia (*24*).

To test the clinical potential of targeting the CD73-A2AR adenosinergic pathway, we used a combined CD73 Ab-mediated blocking/A2AR inhibition strategy and observed a significant increase in survival of mice transplanted with Lp30 AML cells. The lack of pronounced efficacy of CD73 or A2AR targeted monotherapies has also been observed in solid tumor models and may involve pharmacokinetics issues of the CD73 Ab, which is optimized for human use (*39*, *43*). We also note that the Ab isotype is an important parameter in our setting, as only the IgG2A and not the IgG1 isotype displayed therapeutic benefit (data not shown), perhaps reflecting the higher FcγR binding capacity of the former. Similar findings have been made in the context of solid cancers (*39*).

In conclusion, our work provides novel insights on how an isoform switch in a key myeloid TF drives a leukemic-specific transcriptional program, ultimately resulting in AML. We furthermore identify CD73 and A2AR as potential targets in biallelic *CEBPA* mutant AML via their ability to stimulate autocrine adenosinergic signaling. This contrasts observations in solid cancers, where CD73-mediated suppression of the adaptive immune system seems to be the main function of CD73 as a tumor-promoting factor (*35*, *36*, *44*), perhaps reflecting different physical properties of leukemic versus solid cancer niches. Currently, a number of agents targeting CD73 and the adenosinergic pathway are being evaluated for their efficacy against a variety of solid cancers in early clinical trials, either as single agents or in combination with immune modulatory therapies such as anti-PD1 or anti-PDL1 (*45*). Another intriguing possibility is the combination with Janus kinase inhibitors, shown recently to be a potential *CEBPA* mutant targeted therapy (*46*). On the basis of the findings in the present work, we suggest that such emerging treatment strategies should also be evaluated in the context of *CEBPA* mutant AML.

MATERIALS AND METHODS

Experimental design

To identify CEBPA-bound putative enhancers specific for *CEBPA* mutant AML, we performed microscale, in vivo ChIP-seq on sorted leukemic GMPs and their WT counterparts. RNA-seq was carried out to identify gene expression changes in human *CEBPA* mutant AML and the corresponding *Cebpa*^{Lp30} mouse model, leading to the identification of *Nt5e*, encoding CD73, as a cross-species AML gene. Functional validation of CD73 as a druggable tumor-promoting factor was carried out by shRNA or dCas9-KRAB–mediated KD or pharmacological inhibition followed by BMT.

BMT, mouse

All BMTs were carried out on sublethally irradiated 10- to 15-week-old female B6-SJL recipients by intravenous tail vein injections. For a detailed description of different experimental setups, see Supplementary Materials and Methods. The *Cebpa*^{Lp30} mice were described in (*11*). All mouse experiments were conducted according to protocols approved by the Danish Animal Ethical Committee (permission #2013-15-2934-00780), with regard to the three R's (refine, reduce, and replace) of animal experiments. Animals were housed in individually ventilated cages, and all experiments were carried out under supervision of veterinarians of the Department of Molecular Medicine, University of Copenhagen.

Patients with AML and healthy controls, BM collection

BM cells were aspirated from the posterior iliac crest of healthy subjects and patients with de novo AML before treatment. This study was performed in accordance with the Declaration of Helsinki under the following ethical approvals: Copenhagen, H-15004577; Aarhus, M-20070171; London, 10/H0704/65-006650QM; and Ulm, 148/10.

Primary cultures and cell lines

Lp30 cells were generated by serial BMT/expansion of BM cells from leukemic primary *Cebpa*^{Lp30} mice. A pool of BM cells from tertiary expansions were used for both in vitro and in vivo experiments. BM cells were harvested from femur, tibia, and iliac bones; crushed; washed; pooled; and frozen in vials.

For in vitro proliferation, cell cycle, and apoptosis assays, Lp30 cells (female) were grown in R20/20 media: RPMI 1640 medium (Life Technologies) supplemented with 20% WEHI conditioned media, 20% fetal bovine serum (FBS), 1% penicillin/streptomycin (Pen/Strep), and cytokines (PeproTech): stem cell factor (SCF) (20 ng/ml) and hIL-6 (10 ng/ml). A2AR inhibitor (SCH58264, Sigma-Aldrich) was added from stock (5 mg/ml) in dimethyl sulfoxide (DMSO) to 30, 10, or 3 μM, and DMSO volume was normalized/added as mock.

BM cells from recipients transplanted with donor BM cells from *Cbfb-MYH11* and *KIT* D816 mutant mice [*Cbfb*$^{+/56m}$; *Tg(Mx1-Cre)/KIT*$^{D816Y/V}$] [referred to as Inv(16) cells] (*47*) were grown in x-vivo complete media: X-VIVO 15 with gentamicin (Lonza), supplemented with 10% bovine serum albumin (BSA) (Stem Cell Technologies), 0.1 mM β-mercaptoethanol (Sigma-Aldrich), 1% L-glutamine (Gibco), 1% Pen/Strep, and cytokines (PeproTech): mSCF (50 ng/ml), hIL-6 (50 ng/ml), mIL-3 (10 ng/ml), and GM-CSF (10 ng/ml). Phoenix and HEK293T (human embryonic kidney line, female) cells were cultured in DMEM (Life Technologies) + 10% FBS and 1% Pen/Strep.

All cell cultures were mycoplasma-tested before freezing and never kept in culture for more than 3 months after rethawing. Phoenix and HEK293T cells were the only commercially available cell lines used, and virus production served as authentication of these cell lines.

Proliferation assays [Lp30 and Inv(16) cells]

Cells were plated at equal concentrations with varying concentrations of the inhibitor and in triplicate wells. Cells were counted, the concentration was calculated every second/third day, and the cells

were replated at even cell concentrations. A growth curve was plotted for cumulative growth according to the dilution at each time point. Doubling time was calculated from fitted semi-logarithmic slope (Nonlin). Fit using least squares in GraphPad Prism software by $\log_2$/slope and Student's two-tailed *t* test was used to test for significance. For cell cycle assays (Lp30 cells), cells were plated with 30 μM inhibitor or DMSO for 24 hours. Cells were harvested, and an equal number of cells were fixed in 2% paraformaldehyde, permeabilized in 0.1% saponin, stained with 4′,6-diamidino-2-phenylindole (DAPI), and analyzed by flow cytometry (LSR-II, BD Biosciences). For apoptosis assay (Lp30 cells), cells were plated with 30 μM inhibitor or DMSO for 72 hours, harvested, washed and stained using a PE-annexin V kit (BD Biosciences), and analyzed by flow cytometry (Accuri, BD Biosciences). All flow cytometry analyses were run with FlowJo software V.10.

Retro- and lentiviral transductions

sgRNA nucleotides were cloned into pLKO5-sgRNA-EFS-GFP (Addgene) as described in (*48*) with Bsm BI digestion. pLKO5-sgRNA-EFS-GFP and pHR-SFFV-KRAB-dCas9-P2A-mCherry (Addgene) were used for lentiviral supernatant production by transfection of HEK cells.

shRNA-mir oligonucleotides were cloned into the pMSCV-LTRmiR30-SV40-GFP vector using Eco RI restriction digest. Retroviral supernatant was produced by transfection of Phoenix-ECO cells.

Expanded, tertiary Lp30 cell vials were thawed and cultured in x-vivo complete media. One day after thawing, cells were transduced twice on two consecutive days by 50-min retro- or lentivirus spin-oculation (2000*g*, 32°C) on RetroNectin (Takara Bio)–treated and 2% BSA (STEMCELL Technologies)–blocked wells, and cells were plated subsequently at 3×10^5 cells per milliliter of X-VIVO^{TM} complete media. For analysis after transduction, cells were resuspended in phosphate-buffered saline (PBS) + 3% fetal calf serum.

Flow cytometry

Analytical stainings were assessed on an LSRII, whereas cell sorting was carried out on either an Aria I or an Aria III (all instruments were from Becton Dickinson). Detailed descriptions of all stainings and gating strategies are provided in Supplementary Materials and Methods.

Western blotting

Flow cytometry–sorted GMPs (see above) from leukemic Lp30 and WT mice, corresponding to approximately 10,000 cells for each sample, were boiled in SDS-loading buffer for 5 min, subjected to nucleic acid degradation by Benzonase (E1014-5KU, Sigma-Aldrich) for 20 min on ice, and spun for 20 min at 20,000*g*. Material was size-separated using NuPAGE precast 4 to 12% Bis-tris gels (Invitrogen). The Cell Signaling protocol (www.cellsignal.com/support/protocols/western.html) was used for blotting. ImageJ was used for quantifications using program guidelines (http://rsb.info.nih.gov/ij/). CEBPA Ab [at 1:1000 dilution in 5% (w/v) BSA, 1 hour at room temperature] corresponds to the one used for ChIP (clone 14AA, sc-61, Santa Cruz Biotechnology), and loading control was anti-Histone H3 [1:5000 in 5% (w/v) nonfat milk blocking buffer, 2 hours at room temperature; Ab10799, Abcam]. A high-sensitivity chemiluminescence HRP detection kit was used (Amersham ECL Prime Western Blotting Detection Reagent, RPN2232).

Transient transfection/dual luciferase assay

Luciferase assays were performed according to the kit manufacturer protocol (cat# E1910, Promega). Briefly, 15,000 HEK293 cells were plated in a white-bottom 96-well tissue culture plate. The following day, 0.2 ng of *Renilla* control vector (pRL-CMV, cat# E2261, Promega), 20 ng of empty or enhancer-containing promotor-pGL4 (pGL4:23, cat# E841A, Promega), and 20 ng of either empty or CEBPA-construct containing pcDNA3 (MSC-154) (Thermo Fisher Scientific) vector were transfected using a 3:1 μl/μg ratio of TransIT-2020 (MIR 5404, Mirus) reagent. After a 24-hour incubation, readouts were obtained using a standard luminometer. Constructs used include pcDNA3-Cebpa(WT) and pcDNA3-Cebpa(p30) expression constructs, and pGL4:23 containing human and mouse putative *NT5E/Nt5e* enhancers cloned to the multiple cloning site with the primers listed in data file S7. The human enhancer was first cloned to the TOPO vector (pCR-2.1-Topo, K450002, Thermo Fisher Scientific) and then cloned using Kpn I and Xho I restriction enzymes. The mouse enhancer was cloned directly from PCR with the same restriction enzymes.

mRNA–RT-qPCR expression analysis

For expression analysis, cells were sorted as described above, RNA-extracted using the RNeasy Micro Kit (QIAGEN) or NucleoSpin RNA XS (MN), and reverse-transcribed to cDNA using the ProtoScript First Strand cDNA Synthesis Kit (M-MuLV) and oligo (dT) primers (NEB). RT-qPCR was performed using LightCycler 480 SYBR Green I Master (Roche Life Sciences). Data were normalized to *Actg1* (mouse) or *POL2AR* and *H6PD* (human). Primers used are listed in data file S7.

Preparation of human cDNA libraries and sequencing

Total RNA was extracted from GMPs using the RNeasy Micro Kit (QIAGEN). Thirty nanograms of RNA was processed for double-stranded cDNA synthesis with the Ovation RNA-Seq System V2 (NuGEN Technologies). Subsequently, 1 μg of the sheared cDNA [fragment size, 200 to 600 base pairs (bp)] was subjected to library preparation according to the Illumina TruSeq DNA Sample Preparation Kit (ref #15012999) protocol. The indexed libraries were pooled in equimolar ratios and subjected to 100-bp paired-end sequencing on the Illumina HiSeq 2000 system.

Preparation of Lp30 cDNA libraries and sequencing

Recipient mice were transplanted with shRNA-transduced Lp30 cells (1.5×10^6 for each *Nt5e* knockdown construct and 0.5×10^6 for scrambled control). Three weeks after BMT, 5×10^5 GFP-sorted cells from two or three individual mice per construct were used for mRNA extraction (RNeasy mini kit, QIAGEN), and cDNA library was generated using 600 ng of input RNA (TruSeq Library RNA Prep Kit v2, Illumina). Libraries were diluted and sequenced (NextSeq, Illumina).

Mapping and quantification of RNA-seq data

See Supplementary Materials and Methods for detailed description.

Mass spectrometry

Detailed description of the procedure can be found in Supplementary Materials and Methods. Briefly, FACS-sorted cells were washed twice with ice-cold PBS and lysed in 6 M guanidinium hydrochloride, 10 mM tris(2-carboxyethyl)phosphine, 40 mM 2-chloroacetamide, and 100 mM tris (pH 8.5). Proteins were digested first with LysC and subsequently with trypsin at 37°C. Enzyme activity was quenched by trifluoroacetic acid (TFA) at a final concentration of 1%. Before mass spectrometry (MS) analysis, the peptides were desalted on in-house packed C18 StageTips. Samples were analyzed in a label-free manner, where each sample was loaded onto a 2-cm C18 trap column,

connected in line to a 50-cm C18 reverse-phase analytical column (Easy-Spray ES803, Thermo Fisher Scientific). Peptides were eluted over a 200-min gradient, ranging from 5 to 48% of acetonitrile at 250 nl/min, and analyzed in a ddMS2-IT-HCD top speed method on an Orbitrap Fusion (Thermo Fisher Scientific). MS performance was verified for consistency by running complex cell lysate quality control standards, and chromatography was monitored to check for reproducibility.

Chromatin preparation and immunoprecipitation

ChIP on both mouse and human samples was performed as described previously (*49*, *50*), with the exception that amplification for the human ChIP samples was done with the New England Biolabs Ultra Amplification Kit (cat# E7370, NEB) and no *Escherichia coli* carrier DNA. Specific washing conditions not mentioned previously include four times low-salt (140 mM NaCl) radioimmunoprecipitation assay (RIPA) buffer washes for both H3K4me1 and H3K27ac precipitations, replacing all high-salt (500 mM) washes [see (*50*) for detailed protocol]. Abs used were CEBPA (clone 14AA, sc-61, Santa Cruz Biotechnology), H3K4me1 (ab8895, Abcam), and H3K27ac (ab4729, Abcam). See primer table (data file S7) for primer sets used for assessing the quality of each individual precipitation.

Mapping and quantification of ChIP-seq data

See Supplementary Materials and Methods for detailed description.

3C-qPCR

3C was done essentially as described previously (*51*) with some modifications. Specifically, mouse Lp30 leukemic GMP cells (Lin^- $cKit^+$ $Sca1^-$ $CD150^-$ $CD41^-$ $FcgRII/III^+$) were isolated by FACS, while $cKit^+$ WT BM cells were isolated by magnetic-activated cell sorting (MACS) (CD117 magnetic microbeads, Miltenyi Biotech) for comparison. Approximately 2 million cells were used per reaction, fixed in 1.5% formaldehyde in 10 ml of cold PBS/RPMI medium 50%/50% rotating at room temperature for 10 min, and quenched for 2 min in 187 mM of added glycine. Lysis was done by douncing (glass) 10 strokes on ice after 15 min of incubation on ice. Cell fragments/nuclei were recovered by centrifugation at 2200*g* for 5 min at 4°C and washed once in ice-cold restriction buffer and resuspended in 0.5 ml of restriction buffer. Chromatin was exposed for digestion by a 1-hour incubation with 0.1% of SDS at 37°C, followed by a 1-hour incubation with 1% Triton X-100 at 37°C. Overnight digestion with 200 U of Xba I (R0145T, NEB) with the addition of 100 U of enzyme for the last 4 hours was followed by 30 min of heat inactivation at 65°C. Ligation was performed with 20,000 U of T4 ligase (M0202T, NEB) for 3 hours at 20°C. DNA was isolated by RNase A (19101, QIAGEN) exposure for 30 min, followed by addition of 1 mg of proteinase K (P6556, Sigma-Aldrich) and incubation in 0.4% SDS for 2 hours and phenol-chloroform extraction using phase-lock tubes (713-2536, 5-prime). RT-qPCR was performed as described above, with quadruplicates for each data point and a high-stringency, 50-cycle program. All primers are listed in data file S7.

Statistical analysis

The statistical analyses used, the definition of what *n* represents, and the meaning of numbers of asterisks are indicated for each experiment in the relevant figure legends. For BMT experiments, recipient mice were randomized to receive control and test leukemic cells, respectively. For survival analysis, individual mice were shuffled between cages. See Supplementary Materials and Methods. No blinding of experimental groups was performed. No statistical method was applied to predetermine sample sizes, but sample sizes are indicated in relevant figures.

SUPPLEMENTARY MATERIALS

Supplementary material for this article is available at http://advances.sciencemag.org/cgi/content/full/5/7/eaaw4304/DC1

Supplementary Materials and Methods

Fig. S1. Distinct enhancer-binding of CEBPA in WT GMPs versus p30 L-GMPs, related to Fig. 1.

Fig. S2. Motif enrichment analysis of p42, common and p30 CEBPA-bound regions, related to Fig. 2.

Fig. S3. Gene expression analysis of murine and human *CEBPA* mutant AML, related to Fig. 3.

Fig. S4. CEBPA-p30 directly activates the expression of *Nt5e*, related to Fig. 4.

Fig. S5. CD73-positive GMPs in human AML and CBF-MYH binding of the *NT5E* promoter in INV(16) AML, related to Fig. 5.

Fig. S6. A2AR-dependent adenosinergic autocrine survival signaling promoted by CD73, related to Fig. 6.

Data File S1. CEBPA-peak coordinates, enriched motifs in CEBPA regions, related to Fig. 1.

Data File S2. RNA-seq data, related to Figs. 2 and 3.

Data File S3. MS data, related to Figs. 2 and 3.

Data File S4. Gene signatures, related to Fig. 3.

Data File S5. RNA-seq data, related to Fig. 6.

Data File S6. Gene signatures, related to Fig. 6.

Data File S7. Materials lists, related to Materials and Methods.

References (*52*–*73*).

REFERENCES AND NOTES

1. E. Papaemmanuil, M. Gerstung, L. Bullinger, V. I. Gaidzik, P. Paschka, N. D. Roberts, N. E. Potter, M. Heuser, F. Thol, N. Bolli, G. Gundem, P. Van Loo, I. Martincorena, P. Ganly, L. Mudie, S. McLaren, S. O'Meara, K. Raine, D. R. Jones, J. W. Teague, A. P. Butler, M. F. Greaves, A. Ganser, K. Döhner, R. F. Schlenk, H. Döhner, P. J. Campbell, Genomic classification and prognosis in acute myeloid leukemia. *N. Engl. J. Med.* **374**, 2209–2221 (2016).
2. Cancer Genome Atlas Research Network, T. J. Ley, C. Miller, L. Ding, B. J. Raphael, A. J. Mungall, A. Robertson, K. Hoadley, T. J. Triche Jr., P. W. Laird, J. D. Baty, L. L. Fulton, R. Fulton, S. E. Heath, J. Kalicki-Veizer, C. Kandoth, J. M. Klco, D. C. Koboldt, K. L. Kanchi, S. Kulkarni, T. L. Lamprecht, D. E. Larson, L. Lin, C. Lu, M. D. McLellan, J. F. McMichael, J. Payton, H. Schmidt, D. H. Spencer, M. H. Tomasson, J. W. Wallis, L. D. Wartman, M. A. Watson, J. Welch, M. C. Wendl, A. Ally, M. Balasundaram, I. Birol, Y. Butterfield, R. Chiu, A. Chu, E. Chuah, H. J. Chun, R. Corbett, N. Dhalla, R. Guin, A. He, C. Hirst, M. Hirst, R. A. Holt, S. Jones, A. Karsan, D. Lee, H. I. Li, M. A. Marra, M. Mayo, R. A. Moore, K. Mungall, J. Parker, E. Pleasance, P. Plettner, J. Schein, D. Stoll, L. Swanson, A. Tam, N. Thiessen, R. Varhol, N. Wye, Y. Zhao, S. Gabriel, G. Getz, C. Sougnez, L. Zou, M. D. Leiserson, F. Vandin, H. T. Wu, F. Applebaum, S. B. Baylin, R. Akbani, B. M. Broom, K. Chen, T. C. Motter, K. Nguyen, J. N. Weinstein, N. Zhang, M. L. Ferguson, C. Adams, A. Black, J. Bowen, J. Gastier-Foster, T. Grossman, T. Lichtenberg, L. Wise, T. Davidsen, J. A. Demchok, K. R. Shaw, M. Sheth, H. J. Sofia, L. Yang, J. R. Downing, G. Eley, Genomic and epigenomic landscapes of adult de novo acute myeloid leukemia. *N. Engl. J. Med.* **368**, 2059–2074 (2013).
3. H. Döhner, E. Estey, D. Grimwade, S. Amadori, F. R. Appelbaum, T. Büchner, H. Dombret, B. L. Ebert, P. Fenaux, R. A. Larson, R. L. Levine, F. Lo-Coco, T. Naoe, D. Niederwieser, G. J. Ossenkoppele, M. Sanz, J. Sierra, M. S. Tallman, H.-F. Tien, A. H. Wei, B. Löwenberg, C. D. Bloomfield, Diagnosis and management of AML in adults: 2017 ELN recommendations from an international expert panel. *Blood* **129**, 424–447 (2017).
4. C. C. Coombs, M. Tavakkoli, M. S. Tallman, Acute promyelocytic leukemia: Where did we start, where are we now, and the future. *Blood Cancer J.* **5**, e304 (2015).
5. P. Zhang, J. Iwasaki-Arai, H. Iwasaki, M. L. Fenyus, T. Dayaram, B. M. Owens, H. Shigematsu, E. Levantini, C. S. Huettner, J. A. Lekstrom-Himes, K. Akashi, D. G. Tenen, Enhancement of hematopoietic stem cell repopulating capacity and self-renewal in the absence of the transcription factor C/EBPα. *Immunity* **21**, 853–863 (2004).
6. S. Pundhir, F. K. Bratt Lauridsen, M. B. Schuster, J. S. Jakobsen, Y. Ge, E. M. Schoof, N. Rapin, J. Waage, M. S. Hasemann, B. T. Porse, Enhancer and transcription factor dynamics during myeloid differentiation reveal an early differentiation block in Cebpa null progenitors. *Cell Rep.* **23**, 2744–2757 (2018).
7. B. J. Wouters, B. Löwenberg, C. A. J. Erpelinck-Verschueren, W. L. J. van Putten, P. J. M. Valk, R. Delwel, Double *CEBPA* mutations, but not single *CEBPA* mutations, define a subgroup of acute myeloid leukemia with a distinctive gene expression profile that is uniquely associated with a favorable outcome. *Blood* **113**, 3088–3091 (2009).
8. E. Taskesen, L. Bullinger, A. Corbacioglu, M. A. Sanders, C. A. J. Erpelinck, B. J. Wouters, S. C. van der Poel-van de Luytgaarde, F. Damm, J. Krauter, A. Ganser, R. F. Schlenk,

B. Löwenberg, R. Delwel, H. Döhner, P. J. M. Valk, K. Döhner, Prognostic impact, concurrent genetic mutations, and gene expression features of AML with *CEBPA* mutations in a cohort of 1182 cytogenetically normal AML patients: Further evidence for *CEBPA* double mutant AML as a distinctive disease entity. *Blood* **117**, 2469–2475 (2011).
9. T. Pabst, M. Eyholzer, J. Fos, B. U. Mueller, Heterogeneity within AML with CEBPA mutations; only CEBPA double mutations, but not single CEBPA mutations are associated with favourable prognosis. *Br. J. Cancer* **100**, 1343–1346 (2009).
10. E. Ohlsson, M. B. Schuster, M. Hasemann, B. T. Porse, The multifaceted functions of C/EBPα in normal and malignant haematopoiesis. *Leukemia* **30**, 767–775 (2016).
11. P. Kirstetter, M. B. Schuster, O. Bereshchenko, S. Moore, H. Dvinge, E. Kurz, K. Theilgaard-Mönch, R. Månsson, T. Å. Pedersen, T. Pabst, E. Schrock, B. T. Porse, S. E. W. Jacobsen, P. Bertone, D. G. Tenen, C. Nerlov, Modeling of C/EBPα mutant acute myeloid leukemia reveals a common expression signature of committed myeloid leukemia-initiating cells. *Cancer Cell* **13**, 299–310 (2008).
12. L. T. Smith, S. Hohaus, D. A. Gonzalez, S. E. Dziennis, D. G. Tenen, PU.1 (Spi-1) and C/EBP alpha regulate the granulocyte colony-stimulating factor receptor promoter in myeloid cells. *Blood* **88**, 1234–1247 (1996).
13. S. Hohaus, M. S. Petrovick, M. T. Voso, Z. Sun, D. E. Zhang, D. G. Tenen, PU.1 (Spi-1) and C/EBP alpha regulate expression of the granulocyte-macrophage colony-stimulating factor receptor alpha gene. *Mol. Cell. Biol.* **15**, 5830–5845 (1995).
14. A. M. Ford, C. A. Bennett, L. E. Healy, M. Towatari, M. F. Greaves, T. Enver, Regulation of the myeloperoxidase enhancer binding proteins Pu1, C-EBP alpha, -beta, and -delta during granulocyte-lineage specification. *Proc. Natl. Acad. Sci. U.S.A.* **93**, 10838–10843 (1996).
15. M. Alberich-Jordà, B. Wouters, M. Balastik, C. Shapiro-Koss, H. Zhang, A. Di Ruscio, H. S. Radomska, A. K. Ebralidze, G. Amabile, M. Ye, J. Zhang, I. Lowers, R. Avellino, A. Melnick, M. E. Figueroa, P. J. M. Valk, R. Delwel, D. G. Tenen, C/EBPγ deregulation results in differentiation arrest in acute myeloid leukemia. *J. Clin. Invest.* **122**, 4490–4504 (2012).
16. H. Zhang, M. Alberich-Jorda, G. Amabile, H. Yang, P. B. Staber, A. Di Ruscio, R. S. Welner, A. Ebralidze, J. Zhang, E. Levantini, V. Lefebvre, P. J. M. Valk, R. Delwel, M. Hoogenkamp, C. Nerlov, J. Cammenga, B. Saez, D. T. Scadden, C. Bonifer, M. Ye, D. G. Tenen, Sox4 is a key oncogenic target in C/EBPα mutant acute myeloid leukemia. *Cancer Cell* **24**, 575–588 (2013).
17. A. D. Friedman, S. L. McKnight, Identification of two polypeptide segments of CCAAT/enhancer-binding protein required for transcriptional activation of the serum albumin gene. *Genes Dev.* **4**, 1416–1426 (1990).
18. C. Nerlov, E. B. Ziff, Three levels of functional interaction determine the activity of CCAAT/enhancer binding protein-alpha on the serum albumin promoter. *Genes Dev.* **8**, 350–362 (1994).
19. N. K. Wilson, S. D. Foster, X. Wang, K. Knezevic, J. Schütte, P. Kaimakis, P. M. Chilarska, S. Kinston, W. H. Ouwehand, E. Dzierzak, J. E. Pimanda, M. F. T. R. de Bruijn, B. Göttgens, Combinatorial transcriptional control in blood stem/progenitor cells: Genome-wide analysis of ten major transcriptional regulators. *Cell Stem Cell* **7**, 532–544 (2010).
20. T. Pabst, B. U. Mueller, P. Zhang, H. S. Radomska, S. Narravula, S. Schnittger, G. Behre, W. Hiddemann, D. G. Tenen, Dominant-negative mutations of CEBPA, encoding CCAAT/enhancer binding protein-α (C/EBPα), in acute myeloid leukemia. *Nat. Genet.* **27**, 263–270 (2001).
21. L. Antonioli, C. Blandizzi, P. Pacher, G. Haskó, Immunity, inflammation and cancer: A leading role for adenosine. *Nat. Rev. Cancer* **13**, 842–857 (2013).
22. P. A. Beavis, J. Stagg, P. K. Darcy, M. J. Smyth, CD73: A potent suppressor of antitumor immune responses. *Trends Immunol.* **33**, 231–237 (2012).
23. V. Salvestrini, R. Zini, L. Rossi, S. Gulinelli, R. Manfredini, E. Bianchi, W. Piacibello, L. Caione, G. Migliardi, M. R. Ricciardi, A. Tafuri, M. Romano, S. Salati, F. Di Virgilio, S. Ferrari, M. Baccarani, D. Ferrari, R. M. Lemoli, Purinergic signaling inhibits human acute myeloblastic leukemia cell proliferation, migration, and engraftment in immunodeficient mice. *Blood* **119**, 217–226 (2012).
24. S. Serra, A. L. Horenstein, T. Vaisitti, D. Brusa, D. Rossi, L. Laurenti, G. D'Arena, M. Coscia, C. Tripodo, G. Inghirami, S. C. Robson, G. Gaidano, F. Malavasi, S. Deaglio, CD73-generated extracellular adenosine in chronic lymphocytic leukemia creates local conditions counteracting drug-induced cell death. *Blood* **118**, 6141–6152 (2011).
25. L. S. Qi, M. H. Larson, L. A. Gilbert, J. A. Doudna, J. S. Weissman, A. P. Arkin, W. A. Lim, Repurposing CRISPR as an RNA-guided platform for sequence-specific control of gene expression. *Cell* **152**, 1173–1183 (2013).
26. R. G. W. Verhaak, B. J. Wouters, C. A. J. Erpelinck, S. Abbas, H. B. Beverloo, S. Lugthart, B. Löwenberg, R. Delwel, P. J. M. Valk, Prediction of molecular subtypes in acute myeloid leukemia based on gene expression profiling. *Haematologica* **94**, 131–134 (2009).
27. A. Kohlmann, C. Schoch, S. Schnittger, M. Dugas, W. Hiddemann, W. Kern, T. Haferlach, Molecular characterization of acute leukemias by use of microarray technology. *Genes Chromosomes Cancer* **37**, 396–405 (2003).
28. A. Mandoli, K. Prange, J. H. A. Martens, Genome-wide binding of transcription factors in inv(16) acute myeloid leukemia. *Genom. Data* **2**, 170–172 (2014).
29. B. E. Bernstein, J. A. Stamatoyannopoulos, J. F. Costello, B. Ren, A. Milosavljevic, A. Meissner, M. Kellis, M. A. Marra, A. L. Beaudet, J. R. Ecker, P. J. Farnham, M. Hirst, E. S. Lander, T. S. Mikkelsen, J. A. Thomson, The NIH Roadmap Epigenomics Mapping Consortium. *Nat. Biotechnol.* **28**, 1045–1048 (2010).
30. B. M. Javierre, O. S. Burren, S. P. Wilder, R. Kreuzhuber, S. M. Hill, S. Sewitz, J. Cairns, S. W. Wingett, C. Várnai, M. J. Thiecke, F. Burden, S. Farrow, A. J. Cutler, K. Rehnström, K. Downes, L. Grassi, M. Kostadima, P. Freire-Pritchett, F. Wang, The BLUEPRINT Consortium, H. G. Stunnenberg, J. A. Todd, D. R. Zerbino, O. Stegle, W. H. Ouwehand, M. Frontini, C. Wallace, M. Spivakov, P. Fraser, Lineage-specific genome architecture links enhancers and non-coding disease variants to target gene promoters. *Cell* **167**, 1369–1384.e19 (2016).
31. J. H. A. Martens, H. G. Stunnenberg, BLUEPRINT: Mapping human blood cell epigenomes. *Haematologica* **98**, 1487–1489 (2013).
32. G. Haskó, J. Linden, B. Cronstein, P. Pacher, Adenosine receptors: Therapeutic aspects for inflammatory and immune diseases. *Nat. Rev. Drug Discov.* **7**, 759–770 (2008).
33. S. Gessi, S. Merighi, V. Sacchetto, C. Simioni, P. A. Borea, Adenosine receptors and cancer. *Biochim. Biophys. Acta* **1808**, 1400–1412 (2011).
34. K. E. Barletta, K. Ley, B. Mehrad, Regulation of neutrophil function by adenosine. *Arterioscler. Thromb. Vasc. Biol.* **32**, 856–864 (2012).
35. J. Stagg, U. Divisekera, N. McLaughlin, J. Sharkey, S. Pommey, D. Denoyer, K. M. Dwyer, M. J. Smyth, Anti-CD73 antibody therapy inhibits breast tumor growth and metastasis. *Proc. Natl. Acad. Sci. U.S.A.* **107**, 1547–1552 (2010).
36. D. Jin, J. Fan, L. Wang, L. F. Thompson, A. Liu, B. J. Daniel, T. Shin, T. J. Curiel, B. Zhang, CD73 on tumor cells impairs antitumor T-cell responses: A novel mechanism of tumor-induced immune suppression. *Cancer Res.* **70**, 2245–2255 (2010).
37. B. Allard, M. Turcotte, K. Spring, S. Pommey, I. Royal, J. Stagg, Anti-CD73 therapy impairs tumor angiogenesis. *Int. J. Cancer* **134**, 1466–1473 (2014).
38. L. Wang, J. Fan, L. F. Thompson, Y. Zhang, T. Shin, T. J. Curiel, B. Zhang, CD73 has distinct roles in nonhematopoietic and hematopoietic cells to promote tumor growth in mice. *J. Clin. Invest.* **121**, 2371–2382 (2011).
39. A. Young, S. F. Ngiow, D. S. Barkauskas, E. Sult, C. Hay, S. J. Blake, Q. Huang, J. Liu, K. Takeda, M. W. L. Teng, K. Sachsenmeier, M. J. Smyth, Co-inhibition of CD73 and A2AR adenosine signaling improves anti-tumor immune responses. *Cancer Cell* **30**, 391–403 (2016).
40. C. Cekic, Y.-J. Day, D. Sag, J. Linden, Myeloid expression of adenosine A_{2A} receptor suppresses T and NK cell responses in the solid tumor microenvironment. *Cancer Res.* **74**, 7250–7259 (2014).
41. C. van Oevelen, S. Collombet, G. Vicent, M. Hoogenkamp, C. Lepoivre, A. Badeaux, L. Bussmann, J. L. Sardina, D. Thieffry, M. Beato, Y. Shi, C. Bonifer, T. Graf, C/EBPα activates pre-existing and de novo macrophage enhancers during induced pre-B cell transdifferentiation and myelopoiesis. *Stem Cell Reports* **5**, 232–247 (2015).
42. F. Grebien, M. Vedadi, M. Getlik, R. Giambruno, A. Grover, R. Avellino, A. Skucha, S. Vittori, E. Kuznetsova, D. Smil, D. Barsyte-Lovejoy, F. Li, G. Poda, M. Schapira, H. Wu, A. Dong, G. Senisterra, A. Stukalov, K. V. M. Huber, A. Schönegger, R. Marcellus, M. Bilban, C. Bock, P. J. Brown, J. Zuber, K. L. Bennett, R. Al-Awar, R. Delwel, C. Nerlov, C. H. Arrowsmith, G. Superti-Furga, Pharmacological targeting of the Wdr5-MLL interaction in C/EBPα N-terminal leukemia. *Nat. Chem. Biol.* **11**, 571–578 (2015).
43. D. Vijayan, A. Young, M. W. L. Teng, M. J. Smyth, Targeting immunosuppressive adenosine in cancer. *Nat. Rev. Cancer* **17**, 709–724 (2017).
44. P. A. Beavis, U. Divisekera, C. Paget, M. T. Chow, L. B. John, C. Devaud, K. Dwyer, J. Stagg, M. J. Smyth, P. K. Darcy, Blockade of A_{2A} receptors potently suppresses the metastasis of $CD73^+$ tumors. *Proc. Natl. Acad. Sci. U.S.A.* **110**, 14711–14716 (2013).
45. C. M. Hay, E. Sult, Q. Huang, K. Mulgrew, S. R. Fuhrmann, K. A. McGlinchey, S. A. Hammond, R. Rothstein, J. Rios-Doria, E. Poon, N. Holoweckyj, N. M. Durham, C. C. Leow, G. Diedrich, M. Damschroder, R. Herbst, R. E. Hollingsworth, K. F. Sachsenmeier, Targeting CD73 in the tumor microenvironment with MEDI9447. *Oncoimmunology* **5**, e1208875 (2016).
46. V.-P. Lavallée, J. Krosl, S. Lemieux, G. Boucher, P. Gendron, C. Pabst, I. Boivin, A. Marinier, C. J. Guidos, S. Meloche, J. Hébert, G. Sauvageau, Chemo-genomic interrogation of *CEBPA* mutated AML reveals recurrent *CSF3R* mutations and subgroup sensitivity to JAK inhibitors. *Blood* **127**, 3054–3061 (2016).
47. L. Zhao, J. J. Melenhorst, L. Alemu, M. Kirby, S. Anderson, M. Kench, S. Hoogstraten-Miller, L. Brinster, Y. Kamikubo, D. G. Gilliland, P. P. Liu, *KIT* with D816 mutations cooperates with *CBFB-MYH11* for leukemogenesis in mice. *Blood* **119**, 1511–1521 (2012).
48. F. A. Ran, P. D. Hsu, J. Wright, V. Agarwala, D. A. Scott, F. Zhang, Genome engineering using the CRISPR-Cas9 system. *Nat. Protoc.* **8**, 2281–2308 (2013).
49. T. Sandmann, J. S. Jakobsen, E. E. M. Furlong, ChIP-on-chip protocol for genome-wide analysis of transcription factor binding in *Drosophila melanogaster* embryos. *Nat. Protoc.* **1**, 2839–2855 (2006).

50. J. S. Jakobsen, F. O. Bagger, M. S. Hasemann, M. B. Schuster, A.-K. Frank, J. Waage, K. Vitting-Seerup, B. T. Porse, Amplification of pico-scale DNA mediated by bacterial carrier DNA for small-cell-number transcription factor ChIP-seq. *BMC Genomics* **16**, 46 (2015).
51. H. Hagège, P. Klous, C. Braem, E. Splinter, J. Dekker, G. Cathala, W. de Laat, T. Forné, Quantitative analysis of chromosome conformation capture assays (3C-qPCR). *Nat. Protoc.* **2**, 1722–1733 (2007).
52. M. S. Hasemann, F. K. B. Lauridsen, J. Waage, J. S. Jakobsen, A.-K. Frank, M. B. Schuster, N. Rapin, F. O. Bagger, P. S. Hoppe, T. Schroeder, B. T. Porse, C/EBPα is required for long-term self-renewal and lineage priming of hematopoietic stem cells and for the maintenance of epigenetic configurations in multipotent progenitors. *PLOS Genet.* **10**, e1004079 (2014).
53. C. J. H. Pronk, D. J. Rossi, R. Månsson, J. L. Attema, G. L. Norddahl, C. K. F. Chan, M. Sigvardsson, I. L. Weissman, D. Bryder, Elucidation of the phenotypic, functional, and molecular topography of a myeloerythroid progenitor cell hierarchy. *Cell Stem Cell* **1**, 428–442 (2007).
54. H. Mora-Jensen, J. Jendholm, N. Rapin, M. K. Andersen, A. S. Roug, F. O. Bagger, L. Bullinger, O. Winther, N. Borregaard, B. T. Porse, K. Theilgaard-Mönch, Cellular origin of prognostic chromosomal aberrations in AML patients. *Leukemia* **29**, 1785–1789 (2015).
55. N. A. Kulak, G. Pichler, I. Paron, N. Nagaraj, M. Mann, Minimal, encapsulated proteomic-sample processing applied to copy-number estimation in eukaryotic cells. *Nat. Methods* **11**, 319–324 (2014).
56. J. Rappsilber, M. Mann, Y. Ishihama, Protocol for micro-purification, enrichment, pre-fractionation and storage of peptides for proteomics using StageTips. *Nat. Protoc.* **2**, 1896–1906 (2007).
57. E. E. Wojtowicz, E. R. Lechman, K. G. Hermans, E. M. Schoof, E. Wienholds, R. Isserlin, P. A. van Veelen, M. J. C. Broekhuis, G. M. C. Janssen, A. Trotman-Grant, S. M. Dobson, G. Krivdova, J. Elzinga, J. Kennedy, O. I. Gan, A. Sinha, V. Ignatchenko, T. Kislinger, B. Dethmers-Ausema, E. Weersing, M. F. Alemdehy, H. W. J. de Looper, G. D. Bader, M. Ritsema, S. J. Erkeland, L. V. Bystrykh, J. E. Dick, G. de Haan, Ectopic miR-125a expression induces long-term repopulating stem cell capacity in mouse and human hematopoietic progenitors. *Cell Stem Cell* **19**, 383–396 (2016).
58. S. Li, S. W. Tighe, C. M. Nicolet, D. Grove, S. Levy, W. Farmerie, A. Viale, C. Wright, P. A. Schweitzer, Y. Gao, D. Kim, J. Boland, B. Hicks, R. Kim, S. Chhangawala, N. Jafari, N. Raghavachari, J. Gandara, N. Garcia-Reyero, C. Hendrickson, D. Roberson, J. A. Rosenfeld, T. Smith, J. G. Underwood, M. Wang, P. Zumbo, D. A. Baldwin, G. S. Grills, C. E. Mason, Multi-platform assessment of transcriptome profiling using RNA-seq in the ABRF next-generation sequencing study. *Nat. Biotechnol.* **32**, 915–925 (2014).
59. Y. Liao, G. K. Smyth, W. Shi, The Subread aligner: Fast, accurate and scalable read mapping by seed-and-vote. *Nucleic Acids Res.* **41**, e108 (2013).
60. M. D. Robinson, D. J. McCarthy, G. K. Smyth, edgeR: A bioconductor package for differential expression analysis of digital gene expression data. *Bioinformatics* **26**, 139–140 (2010).
61. S. Anders, W. Huber, Differential expression analysis for sequence count data. *Genome Biol.* **11**, R106 (2010).
62. S. Durinck, Y. Moreau, A. Kasprzyk, S. Davis, B. De Moor, A. Brazma, W. Huber, BioMart and Bioconductor: A powerful link between biological databases and microarray data analysis. *Bioinformatics* **21**, 3439–3440 (2005).
63. A. Dobin, C. A. Davis, F. Schlesinger, J. Drenkow, C. Zaleski, S. Jha, P. Batut, M. Chaisson, T. R. Gingeras, STAR: Ultrafast universal RNA-seq aligner. *Bioinformatics* **29**, 15–21 (2013).
64. D. C. Jones, K. T. Kuppusamy, N. J. Palpant, X. Peng, C. E. Murry, H. Ruohola-Baker, W. L. Ruzzo, Isolator: Accurate and stable analysis of isoform-level expression in RNA-seq experiments. bioRxiv 088765 [**Preprint**]. 20 November 2016. https://doi.org/10.1101/088765.
65. H. Pimentel, N. L. Bray, S. Puente, P. Melsted, L. Pachter, Differential analysis of RNA-seq incorporating quantification uncertainty. *Nat. Methods* **14**, 687–690 (2017).
66. N. L. Bray, H. Pimentel, P. Melsted, L. Pachter, Near-optimal probabilistic RNA-seq quantification. *Nat. Biotechnol.* **34**, 525–527 (2016).
67. A. R. Quinlan, I. M. Hall, BEDTools: A flexible suite of utilities for comparing genomic features. *Bioinformatics* **26**, 841–842 (2010).
68. L. Shen, N. Shao, X. Liu, E. Nestler, ngs.plot: Quick mining and visualization of next-generation sequencing data by integrating genomic databases. *BMC Genomics* **15**, 284 (2014).
69. M. Wahlestedt, V. Ladopoulos, I. Hidalgo, M. Sanchez Castillo, R. Hannah, P. Säwen, H. Wan, M. Dudenhöffer-Pfeifer, M. Magnusson, G. L. Norddahl, B. Göttgens, D. Bryder, Critical modulation of hematopoietic lineage fate by hepatic leukemia factor. *Cell Rep.* **21**, 2251–2263 (2017).
70. D. Karolchik, A. S. Hinrichs, T. S. Furey, K. M. Roskin, C. W. Sugnet, D. Haussler, W. J. Kent, The UCSC Table Browser data retrieval tool. *Nucleic Acids Res.* **32**, D493–D496 (2004).
71. B. Langmead, S. L. Salzberg, Fast gapped-read alignment with Bowtie 2. *Nat. Methods* **9**, 357–359 (2012).
72. E. Cerami, J. Gao, U. Dogrusoz, B. E. Gross, S. O. Sumer, B. A. Aksoy, A. Jacobsen, C. J. Byrne, M. L. Heuer, E. Larsson, Y. Antipin, B. Reva, A. P. Goldberg, C. Sander, N. Schultz, The cBio cancer genomics portal: An open platform for exploring multidimensional cancer genomics data. *Cancer Discov.* **2**, 401–404 (2012).
73. K. Hebestreit, S. Gröttrup, D. Emden, J. Veerkamp, C. Ruckert, H.-U. Klein, C. Müller-Tidow, M. Dugas, Leukemia gene atlas—A public platform for integrative exploration of genome-wide molecular data. *PLOS ONE* **7**, e39148 (2012).

Acknowledgments: We thank A. Fossum for help with cell sorting and members of the Porse lab for discussions. MedImmune provided the anti-CD73 Ab used for in vivo treatment experiments. **Funding:** This study was supported by the Danish Cancer Society, the Danish Association for Cancer Research, and the Novo Nordisk Foundation and through a center grant from the Novo Nordisk Foundation (Novo Nordisk Foundation Center for Stem Cell Biology, DanStem; grant number NNF17CC0027852). The AML tissue bank at Queen Mary University was supported by the Medical College of St. Bartholomew's Hospital Trust. **Author contributions:** J.S.J., L.G.L., M.B.S., Y.G., E.S., C.G., T.D., and J.J. performed the experiments. J.S.J., L.G.L., M.B.S., S.P., E.S., K.V.-S., J.F., K.R., K.T.-M., and B.T.P. analyzed the data. J.S.J., L.G.L., M.B.S., and B.T.P. designed the experiments. P.H., K.D., L.B., and J.F. provided essential clinical material. L.G.L., J.S.J., M.B.S., and B.T.P. drafted the manuscript. All authors have proofread and approved the final version of the manuscript. **Competing interests:** J.S.J. is presently an employee of Symphogen A/S. The remaining authors declare that they have no competing interests. **Data and materials availability:** All data needed to evaluate the conclusions in the paper are present in the paper and/or the Supplementary Materials. All sequencing data can be retrieved at GEO (GSE118963). The MS data have been deposited to the ProteomeXchange Consortium (http://proteomecentral.proteomexchange.org) via the PRIDE partner repository with the dataset identifier PXD011359. Additional data related to this paper may be requested from the authors.

Submitted 19 December 2018
Accepted 31 May 2019
Published 10 July 2019
10.1126/sciadv.aaw4304

Citation: J. S. Jakobsen, L. G. Laursen, M. B. Schuster, S. Pundhir, E. Schoof, Y. Ge, T. d'Altri, K. Vitting-Seerup, N. Rapin, C. Gentil, J. Jendholm, K. Theilgaard-Mönch, K. Reckzeh, L. Bullinger, K. Döhner, P. Hokland, J. Fitzgibbon, B. T. Porse, Mutant CEBPA directly drives the expression of the targetable tumor-promoting factor CD73 in AML. *Sci. Adv.* **5**, eaaw4304 (2019).